Numerical simulation of dynamic earthquake triggering based on rate- and state-dependent friction law

*Shingo Yoshida[1]

1. Earthquake Research Institute, University of Tokyo

Dieterich (1994) represented time to instability as a function of slip velocity assuming single spring-block system based on rate- and state-dependent friction law (RSF), and denoted that increase of the slip velocity due to static stress change triggers earthquakes. We extend this model to the case of dynamic stress change, noting that increment of logarithm of slip velocity is proportional to difference between static stress change and state variable (frictional strength) change. When fault strength is decreased by dynamic stress change due to seismic waves, earthquake occurrence could be advanced, resulting in delayed dynamic triggering even if no static stress change occurs.
We conducted numerical simulations of earthquake triggering assuming a circular asperity obeying RSF law revised by Nagata et al. (2012). In a situation where earthquakes repeatedly occur, we apply dynamic stress disturbance of sinusoidal variation at a certain time. The dynamic stress change causes increase of slip velocity following the RSF law, and resultant slip weakens the frictional strength. This leads to dynamic earthquake triggering depending on the amplitude of the disturbance. When the stress disturbance is sufficiently large, earthquake occurs during the period of stress oscillating. This might correspond to dynamic triggered earthquakes during passage of seismic waves. When static stress is also increased, smaller dynamic disturbance can trigger earthquakes with a shorter delay. Even if static stress change is negative, a certain amplitude of dynamic stress change can trigger earthquakes.
Figure 1 shows relation between the time to instability and the increase of logarithm of the slip velocity at the center of the asperity. Red, blue, and green circles denote triggering due to static stress change, dynamic stress change, and both stress change, respectively.

Keywords: dynamic earthquake triggering

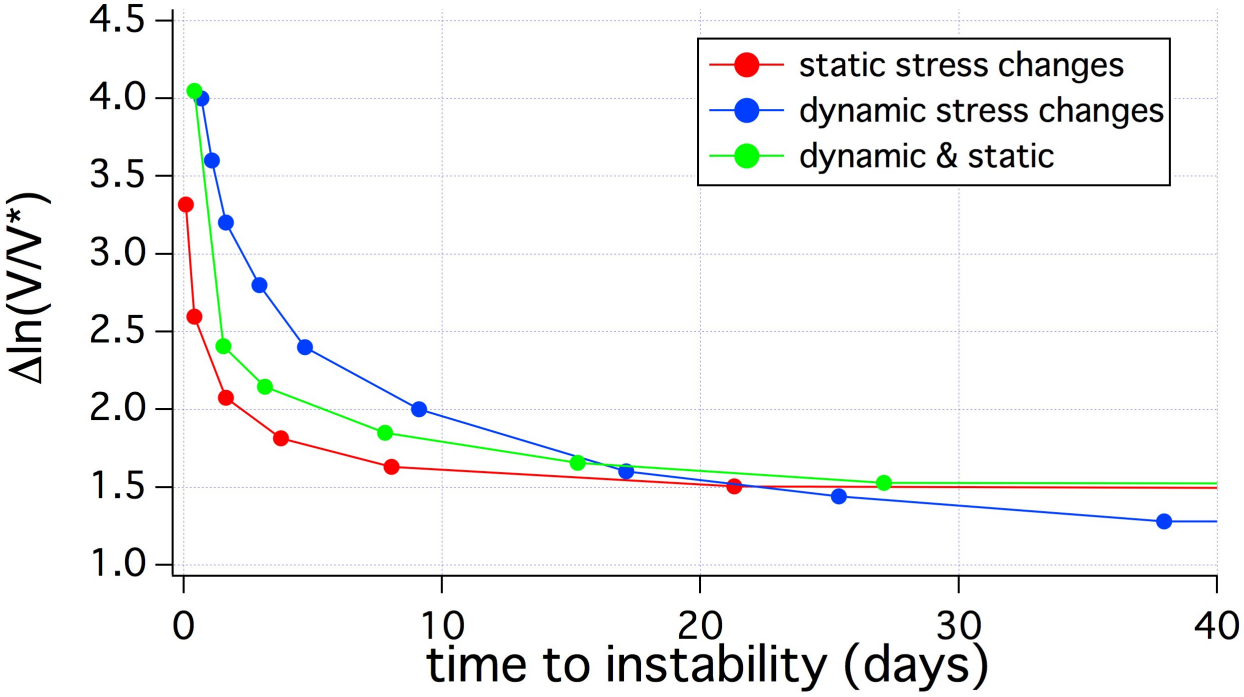

Fig.1

Evaluation of the diffusivity of dissolved ions through grain boundary of quartz and its application to the prediction of frictional healing

*Naoki Nishiyama[1], Hiroshi Sakuma[1]

1. National Institute for Materials Science

Laboratory and field observations have shown that the frictional strength of a fault under stationary contact increases with time (frictional healing). The origin of frictional healing has been often interpreted as due to the increase in real contact area along fault surfaces. This interpretation was supported by the direct observation of increase of contact area of glass plates with time (Dietrich and Kilgore, 1994). Slide-hold-slide (SHS) friction experiments (e.g., Frye and Marone, 2002; Katayama et al., 2015) have suggested that quartz shows relatively strong frictional healing compared to clay minerals and water plays a critical role for the frictional healing. In addition, temperature has a large effect on the frictional healing. The frictional healing is often characterized by the cutoff time (t_c) beyond which the frictional strength shows a linear recovery with the logarithm of time. SHS tests (Nakatani and Scholtz, 2004; Tenthorey and Cox, 2006) have suggested that t_c decreased from 1.2E+3 to 5.9E+1 sec as temperature increased from 200 to 927˚C. A plausible mechanism of rapid healing at high temperature is the enhanced contact area by the pressure solution under hydrothermal conditions (e.g., Tenthorey and Cox, 2006). To test whether the hypothesis can quantitatively explain such a healing behavior, the diffusivity of dissolved ions through intergranular water (intergranular diffusivity) is required for predicting the deformation rate by the pressure solution. The intergranular diffusivity of dissolved ions is, however, poorly constrained (He et al., 2013) because of the difficulty of experimental evaluation. In this study, we calculated the intergranular diffusivity of dissolved Si between quartz surfaces by molecular dynamics (MD) simulations.
In the MD simulations, water molecules and dissolved Si were sandwiched between quartz (1010) surfaces terminated with Si-OH groups. We calculated the diffusivity of dissolved Si in the direction parallel to the quartz surfaces. MD simulations were performed for the thickness of intergranular water from 0.5 nm to 2 nm and temperature from 150 to 350˚C.
As the thickness of intergranular water decreases from 2 to 0.5 nm, the diffusion coefficient of dissolved Si decreases by more than one order of magnitude. The activation energy of intergranular diffusivity ranges from 14 to 30 kJ/mol. Using the obtained intergranular diffusivity with the kinetic model of pressure solution, the increase in grain-to-grain contact area of quartz gauge (ΔA (m^2) were calculated as a function of time. Assuming that the strength recovery ΔT(MPa) is proportional to ΔA, we can calculate ΔT by the relationship of $\Delta T = (\Delta A_r / A_{r0}) C$ (A_{r0}: initial real contact area (m^2), C: cohesive strength (MPa)). Calculated t_c (9.4E+3 s at ˚C and 2.0E+2 s at 927˚C) by using the ΔT and time was roughly consistent with the experimental t_c in the SHS tests. The intergranular diffusivity obtained by this study is useful for extrapolating the relationship between time and strength recovery by SHS tests to natural systems and various time scales.

Keywords: Pressure solution, Frictional healing, Rate- and state-dependent friction law

Influence of swelling on frictional property of smectite gouge

*Jun Kameda[1], Toshihiko Shimamoto[2], Ma Shengli [2]

1. Earth and Planetary System Science Department of Natural History Sciences, Graduate School of Science, Hokkaido University, 2. Institute of Geology, China Earthquake Administration

Smectite is a major component of shallow crustal fault gouges (Vrolijk and van der Pluijm, 1999), and is thought to have large influence on their slip behaviors (e.g., Moore and Lockner 2007; Oohashi et al. 2015). In this study we performed ring-shear friction experiments on water-saturated Na-montmorillonite powders to examine the influence of smectite swelling, one of typical features of smectite, on the frictional property of smectite gouges.
Experiments were conducted using a rotary-shear friction apparatus (Institute of Geology, China Earthquake Administration; Yao et al., 2011; Hou et al., 2012) wtih a variable electrolyte concentrations up to 3*M* NaCl under normal stresses of 1.0 and 2.0 MPa. The SWy-2 powder of 2.5 g and 0.75 g of waters with different salinities were placed and dropped between two solid-cylindrical specimens of Indian gabbro to make ~1 mm thick gouge layer, within a Teflon sleeve holding the gouge. Teflon friction was corrected using an intercept method (Mizoguchi et al. 2007).
The experiments demonstrate that the frictional coefficient shows a peak value at the onset of sliding (0.15~0.5), followed by a gradual decrease to less than 0.1 in all runs. The steady state frictional coefficient is dependent on salinity of pore water, and it is as low as ~0.01 when sheared with distilled water, whereas it increases to ~0.05 with 3*M* NaCl solution. According to the Gouy-Chapman (GC) theory (i.e., interparticle forces arising from the overlap of diffuse electric double layers between the charged plates), the higher swelling pressure is expected in lower salinity condition due to expansion of the diffuse double layers. The application of the extended GC theory proposed by Komine and Ogata (2004) predicts that in-situ swelling pressure of the present gouge sample saturated with distilled water reach as high as ~1.5 MPa, almost equivalent to the normal stress loaded during the test, while the interparticle force is rather attractive in the higher salinity conditions (1.0 and 3.0 *M*) caused by the enhancement of the van der Waals force. These results suggest that the swelling pressure can effectively reduce the effective normal stress exerting on the smectite platelets as argued by Chatterji and Morgenstern (1990), leading to the apparent reduction in the frictional coefficient at lower salinity conditions. Our experiments also indicate that frictional property of smectite-rich gouges is governed by pore fluid physico-chemical conditions in natural fault zones.

Keywords: smectite gouge, swelling, friction experiment

Evaluation of frictional melting in subduction-zone faults on the basis of geochemical analyses of fault rocks

*Tsuyoshi Ishikawa[1], Kohtaro Ujiie[2]

1. Kochi Institute for Core Sample Research, Japan Agency for Marine-Earth Science and Technology, 2. Faculty of Life and Environmental Sciences, University of Tsukuba

Pseudotachylytes (solidified frictional melts produced during seismic slip) found in exhumed accretionary complexes are considered to have formed originally at seismogenic depths, and help our understanding of the dynamics of earthquake faulting in subduction zones. The frictional melting should affect rock chemistry. Here, toward better understanding of the frictional melting using chemical means, we carried out detailed major and trace element and Sr isotope analyses for pseudotachylyte-bearing dark veins and surrounding host rocks. The samples collected from the Mugi area of the Shimanto accretionary complex, which were previously investigated by Ujiie et al. (2007 JSG), were used. About one milligram each of samples was collected from a rock chip along the microstructure by using the PC-controlled micro-drilling apparatus, and then analyzed by ICP-MS and TIMS. Host rocks showed a series of compositional trends controlled by mixing of detrital sedimentary components. Unaltered part of the pseudotachylyte vein, on the other hand, showed striking enrichment of fluid-immobile trace elements, consistent with selective melting of fine-grained, clay-rich matrix of the fault rock. Importantly, completely altered parts of the dark veins exhibit essentially the same characteristics as the unaltered part, indicating that the trace element composition of the pseudotachylyte is well preserved even after considerable alteration in the later stages. These results demonstrate that trace element and structural analyses are useful to detect preexistence of pseudotachylytes resulting from selective frictional melting of clay minerals. It has been controversial that pseudotachylytes are rarely formed or rarely preserved. Geochemical analyses on clay-rich localized slipping zones shed light on this topic.

Keywords: earthquakes, fault rocks, frictional melting, geochemistry, subduction zones

Estimation of frictional heating temperature of ancient mega-splay faults in the Cretaceous Shimanto accretionary complex, SW Japan

*Masaki Oku[1], Hideki Mukoyoshi[1], Shunya Kaneki[2], Tetsuro Hirono[2]

1. Department of Geoscience Interdisciplinary Graduate School of Science and Engineering, Shimane University, 2. Graduate school of science, Osaka University

Subduction zone earthquake is generated by activity of plate boundary megathrust and out-of- sequence thrust (OOST) which branch from the deep portion of the megathrust. It is very important to understand the mechanism of subduction-zone earthquake because most of earthquakes larger than M8 in the world are occurred around subduction zones. Although direct observation of fault rocks in seisomogenic zone is necessary to understand earthquake mechanism, collection of present days fault rocks of megathrust and OOST in seismogenic zone is technologically impossible. Recent study revealed that ancient seismogenic subduction faults are exposed on onland accretionary complexes such as Shimanto accretionary complexes. These faults will provide important information about the characteristics of fault rocks. Estimation of maximum temperature recorded in the fault rock provide us slip parameters during an earthquake because frictional heating temperature is directly related to shear stress and slip distance. Pseudotachylyte is discovered along an ancient OOST in the Shimanto accretionary complexes by previous study. Frictional heating temperature of pseudotachylyte is estimated to 650-1100˚C from mineralogical analysis. On the other hand, frictional heating temperature of most of “pseudotachylyte-less” OOSTs is not estimated because of lack of melted minerals. In recent years, Raman analysis of carbonaceous material (CM) in fault rock is used for estimation of frictional heating temperature of faults. The objective of this study is to estimate the frictional heating temperature of pseudotachylyte-less OOSTs in the Shimanto accretionary complex based on the Raman analysis of CM in the fault rocks. This study area is located on the southern coastal line of the Otsuzaki Peninsula, Kochi Prefecture, Japan. In this area, the Late Cretaceous Shimotsui Formation, Kure Melange and Nonokawa Formation is exposed. The Nonokawa and Shimotsui Formation consist of alteration layers of sandstone and shale. The Kure Mélange is composed of shale with blocks of sandstone, chert and basaltic rocks. More than 18 branched OOSTs are exposed along the southern coastal line of the Otsuzaki Peninsula. Strike of the OOSTs is generally NW and dip is 30˜60˚ NE. Composite planner fabric of Y plane and P plane which indicates reverse fault shear sense is observed in each faults. Samples of fault rocks was collected from four faults (named F1 to F4) and polished slab and thin section of each faults is prepared for detailed observation and Raman analysis. Principal slip zone of each fault was selected for making thin section. Raman spectra analysis was conducted by Horiba Xplora Raman spectrometer installed in the Osaka University. CM in the fault zone and host rock was identified by the microscopic observation and Raman spectra of each CMs were measured. Raman parameter of intensity ratio of D and G bands (ID/IG) and area ratio of D and G bands (AD/AG) was determined for the temperature estimation. Shape of each spectrum was also carefully observed. Heating temperature was estimated by comparing the determined Raman parameter with reported values of heating experiment. Raman parameter of heating experiment reported by previous study show no significant ID/IG change below than 600˚C (in the range of 0.60 from0.57). In contrast, ID/IG values of experimentally heated CM higher than 700˚C drastically increased. Raman parameter of ID/IG and AD/AG of fault zone did not show any systematic change indicating measured faults were not experienced maximum frictional heating temperature higher than 700˚C. However, Raman spectra of host rock and fault zone of F1 fault show systematic change and these shape is similar with those of heating experimented CM of 600˚C.Thus we conclude that the F1 fault experienced a frictional temperature of 600˚C while sliding.

Keywords: Mega splay fault, Raman analysis

Detection of increased heating and estimation of coseismic shear stress from Raman spectra of carbonaceous material in pseudotachylytes

*Keisuke Ito[1], Kohtaro Ujiie[2], Hiroyuki Kagi[3]

1. University of Tsukuba, 2. Graduate School of Life and Environmental Sciences, University of Tsukuba, 3. Geochemical Research Center, Graduate School of Science, The University of Tokyo

Frictional heat generated during earthquakes provides insight into the coseismic fault strength. To detect increased heating associated with faulting at seismic slip rates, we analyzed the Raman spectra of carbonaceous material in natural and experimental pseudotachylytes derived from argillite. The results indicate that the increased carbonization in pseudotachylytes relative to the host rocks could be detected when the ambient temperature is lower than 280 ˚C. This increased carbonization can occur in ~4–16 s and is preserved even after alteration of pseudotachylytes. The comparison between experiment and Raman data demonstrated that there is a correlation between the average shear stress and the Raman spectra in pseudotachylytes. The average coseismic shear stress estimated from the correlation was 1.8 MPa. The resulting apparent friction coefficient under hydrostatic conditions at depths of 4–6 km was ~0.03–0.05. Raman analysis of carbonaceous material-bearing pseudotachylytes will be useful for estimation of coseismic fault strength.

Ito, K., K. Ujiie, and H. Kagi (2017), Detection of increased heating and estimation of coseismic shear stress from Raman spectra of carbonaceous material in pseudotachylytes, *Geophys. Res. Lett.*, in press.

Keywords: carbonaceous material, Raman spectra, pseudotachylyte, frictional heating, coseismic shear stress

Experimental evidence for effects of heating rate on thermal maturation process of carbonaceous materials during earthquake slip

*Shunya Kaneki[1], Tetsuro Hirono[1]

1. Graduate School of Science, Osaka University

Quantitative estimation of frictional heat produced in the fault zone is one of the keys to understand the slip behaviors of an earthquake. Irreversible thermal maturation process of carbonaceous materials, which is very sensitive to maximum temperature, is reported to be a great indicator for frictional heat. In fact, such maturation process could be strongly affcted by not only ambient temperature but also heating rate. However, several previous studies have only conducted heating experiments with heating rate of ~1 ˚C s^{-1} to detect heat recorded in fault rocks, which is markedly lower compared to that of earthquake slip (several tens to several hundreds of degrees per second).
In this study, we have conducted heating experiments with two different heating rate (~1 and ~100 ˚C s^{-1}) on carbonaceous materials retrieved from an ancient plate-subduction fault, and carried out IR and Raman spectroscopies, and py-GC/MS analysis to examine whether heating rate could affect the maturation process of carbonaceous materials. Results showed that maturity of carbonaceous materials after heating with 100 ˚C s^{-1} is lower than that after heating with 1 ˚C s^{-1}. By performing numerical simulation based on one-dimentional thermal diffusion equation, we have re-evaluated maximum temperature of the targeted fault to possibly reach 900 ˚C during past earthquakes, which is much higher than that estimated in the previous study (600 ˚C). We concluded that maturation of carbonaceous materials is strongly affected by heating rate, and such effects must be considered when we estimate maximum temperature from carbonaceous materials.

Keywords: Frictional heat, Carbonaceous materials, Heating rate, Spectrometry

Mechanochemical effects on maturation of carbonaceous materials in faults during earthquakes

*Ichiba Tatsuya[1], Shunya Kaneki[1], Tetsuro Hirono[1], Kiyokazu Oohashi[2]

1. Osaka University Graduate School of Science, 2. Yamaguchi University Faculty of Science Department of Geosphere Sciences

Frictional heating is thought to occur during an earthquake and the shear stress can be estimated from the temperature recorded in the fault. A new temperature proxy for maturity of carbonaceous materials by using infrared and Raman spectroscopies was recently proposed, but intra-crystal change by shear damage may affect on the maturation. Here we focus on the mechanochemical effect in the process by performing low-velocity friction experiment and spectroscopic analyses.

We performed the friction experiments at 3.0 MPa normal stress and 1 mm/s slip rate, and 10 m slip distance by using the mixture of 90 wt.% quartz and 10 wt.% coal. To reproduce heating during earthquake slip, we heated the samples after experiments at 100-1000 ˚C. By comparing the spectra on these samples, we confirmed that some reactions, such as breakage of aliphatic chain, occurred at relatively low temperature on sheared samples. Thus, the mechanochemical effect should be considered for deterring the temperature recorded on the basis of the maturation.

Keywords: Fault, Carbonaceous materials, Spectroscopic analysis

Sintering on a fault during an earthquake

TONOIKE NAOYA[1], *Tetsuro Hirono[1]

1. Department of Earth and Space Science, Graduate School of Science, Osaka University

Frictional heating on a fault during earthquale slip induces various phenomena such as melting, thermal decomposition, and so on. In the case of the Taiwan Chelungpu fault which slipped at the 1999 Chi-Chi earthquake, disk-shaped black material was discovered within the fault zone, and was considered as a pseudotachylite on the basis of the development of hourglass and bubble structures. However, such structures are commonly observed in ceramisc. Here we demonstrated experimentary the sintering phenomenon on the syntetic and natural samples (montmorillonite, illite, and sedimentary host rock nearby the Chelungpu fault). We observed similar structure in the sample that heated at 800 C to those in the fault material. Thus, frictional heating induces not only melting but also sintering, which might affect the frictional behavior and strength recovery of a fault.

Keywords: Sintering, Fault

Experimental measurements and numerical analyses about the temperature change of rocks with stress chang

*Xiaoqiu Yang[1], Weiren Lin[2,3], Osamu Tadai[4], Xin Zeng[1]

1. South China Sea Institute of Oceanology, Chinese Academy of Sciences, 2. Graduate School of Engineering, Kyoto University, 3. Kochi Institute for Core Sample Research, Japan Agency for Marine-Earth Science and Technology (JAMSTEC), 4. Marine Works Japan Ltd.

The temperature responses of rocks to stress changes are key to understanding temperature anomalies in geoscience phenomena such as earthquakes. We developed a new hydrostatic compression system in which the rock specimen center can achieve adiabatic conditions during the first ~10 s following rapid loading or unloading, and systematically measured the representative lithologies of several sedimentary, igneous and metamorphic rocks sampled from two seismogenic zones (the Longmenshan Fault Zone in Sichuan, and the Chelungpu Fault Zone (TCDP Hole-A) in Taiwan), and several quarries worldwide. And we built a finite element model of heat conduction to confirm the measured results of temperature response of rocks to stress change. The results show that: (1) the adiabatic pressure derivative of the temperature (β) for most crustal rocks is ~1.5 to 6.2 mK MPa^{-1}, (2) the temperature response of sedimentary rocks (~3.5 to 6.2 mK MPa^{-1}) is larger than that of igneous and metamorphic rocks (~2.5 to 3.2 mK MPa^{-1}), and (3) there is a good linear correlation between β (in mK MPa^{-1}) and the bulk modulus K (in GPa): $\beta=(-0.068\cdot K+5.69)\pm0.4$, $R^2=0.85$. This empirical equation will be very useful for estimating the distribution of β in the crust, since K can be calculated when profiles of crustal density (ρ) and elastic wave velocities (V_p, V_s) are obtained from gravity surveys and seismic exploration.

Keywords: Adiabatic pressure derivative of temperature (β), Temperature response, Stress change, Hydrostatic compression system, Numerical simulating

Scaly fabrics and veins of the Mugi and Makimine mélanges

*Gabrielle Elizabeth Ramirez[1], Donald M Fisher[1], Gaku Kimura[2], Asuka Yamaguchi[2]

1. Department of Geosciences, Pennsylvania State University, University Park, PA, 2. Department of Earth and Planetary Science, The University of Tokyo, Tokyo, Japan

Ancient subduction fault zones provide a microstructural record of the plate boundary deformation associated with underthrusting. The Mugi and Makimine mélanges of the Shimanto Belt exhibit many of the characteristics associated with exposed ancient subduction fault zones worldwide, including: (1) σ_1 that is near orthogonal to the deformation fabric (2) microstructurally pervasive veins that record hydrofracturing and act as sinks for silica, calcite, and albite (3) cyclic fracturing and sealing recorded through crack-sealing and (4) evidence for local diffusion of silica sourced from web-like arrays of slip surfaces (i.e., scaly fabrics). We present microprobe observations of scaly fabrics and veins from two ancient subduction-related shear zones that represent the full temperature range of the seismogenic zone: 1) Mugi mélange lower (~130-150˚C) and upper (~170-200˚C) sections and 2) Makimine mélange (peak temperatures of ~340˚C). The Mugi mélange is an underplated duplex consisting of two horses separated by an out of sequence thrust fault. The upper section is bounded at the top by a pseudotachylite-bearing paleodécollement. The Makimine mélange was underplated at the downdip limit of the seismogenic zone. The scaly fabrics and veins associated with these shear zones exhibit evidence for different geochemical reactions occurring as a function of depth and temperature. Upper Mugi (170-200 ˚C) has evidence for the incongruent pressure solution reaction of coarse grained albite in the matrix breaking down into illite in the shear zone (i.e. scaly fabric). Makimine (up to ~340 ˚C) has evidence for a different set of reactions that result in rutile and iron-oxide phases concentrated in the shear zone. Microstructural analyses of ancient subduction-related faults show differences with temperature that highlight the importance of establishing the geochemical processes and activation energies that contribute to slip, fracturing, and healing of rocks that underthrust the subduction interface.

Keywords: tectonic mélange, hydrofractures, seismogenic zone, earthquakes

Earthquake magnitude and moment magnitude: Apparent fracture energy and damage zone thickness of faults

*Kiyohiko Yamamoto

Introduction: The relationships between the seismic energy E_s and the magnitude M_s and between the seismic moment M_o and the moment magnitude M_w, respectively, are usually expressed by the following equations.

Log E_s=1.5M_s+4.8 (1)

Log M_o=1.5M_w+9.1 (2)

Hereafter, we call the earthquake that almost follows these equations as the standard earthquake. M_s is smaller than M_w for the relatively large earthquakes along the Japan Trench. In the previous conference, Yamamoto shows the possibility that this difference is elucidated in terms of the seismic efficiency η. On the other hand, (M_j-M_w)>0.2 is found for many intra-earthquakes. For example, (M_j, M_w) is (7.3, 6.9) for the 1995 Hyogo ken Nanbu Earthquake, (7.3, 6.8) for the 2000 Tottori ken Seibu Earthquake, and (7.2, 6.8 to 6.9) for the 2008 Iwate-Miyagi Nairiku Earthquake. For these earthquakes, (M_s-M_w)>0.2, provided M_j = M_s. According to the uniform DMF-model, M_w>M_s when the seismic efficiency η is 0.8 or less, M_ws for η>0.8, and (Ms-Mw)=0.2 at η=1, for the standard earthquake. This implies that the earthquakes of M_s-M_w>0.2 cannot be explained as the standard earthquake. In the present study, we will investigate the causes of (M_s-M_w)>0.2 besides η.

Apparent fracture energy: The damage zone fault (DMF)-model means that a fault has a finite thickness and consists of a damage zone (DZ) area and an asperity (AS) area. In the model, as a slip plane propagates in a DZ area, rotation of the DZ takes place. The apparent fracture energy is equivalent to the work done against the normal stress by the normal displacement to the fault plane due to the rotation. It is assumed that AS has the same rigidity μ and shear fracture strength t_f as the matrix and that DZ is completely relaxed. The uniform DMF model means the fault that has infinite length and uniform thickness. The non-uniform DMF model does the fault with a finite length and non-uniform thickness.

Results: From the uniform DMF-mode, the followings are obtained: 1) Es=(δt/2μ)M_o at η = 1. Here, δt is the stress drop amount. 2) The fraction ϕ of AS area in the fault plane is determined only by the critical strain e_f=t_f/μ and η. Thus, ϕ=(2xe_f) and δt is (2xe_f)x(t_f) at η=1. When e_f is set to 1.5×10^{-2}, (M_s-M_w) becomes approximately 0.2 at η=0.8. A larger value of t_f may be a possible explanation of (Ms-Mw)>0.2 in the case of uniform DMF-model.

Generally, a fault zone has a finite length and non-uniform thickness. The slip propagation requires the stress concentration at the tip of slip plane. It is assumed that the slip amount required for the slip propagation is equal to that of the critical weakening displacement that is necessary for the fracture of AS, and that the slip amount is constant throughout DZ. It is found that as the DZ thickness decreases to zero, the apparent fracture energy approaches twice the strain energy accumulated in AS, per unit area. This suggests that the slip propagation most likely is suppressed when the tip of the slip goes into the DMZ thinner than that around AS. This makes the fault area small compared with that of a standard earthquake for the same AS size, and this makes δt larger. This is another explanation.

Conclusion: (Ms-Mw)> 0.2 occurs in the following cases. 1) For a standard earthquake, the seismic wave efficiency is 0.8 or more. 2) The average stress drop amount is larger than that of a standard earthquake. The larger stress drop amount is caused by the reasons as follows 2-1) the shear fracture strength of AS is larger than the case of standard earthquake, 2-2) the damage zone thickness is small outside the AS area. This means a case where the fault plane is geometrically non-uniform. The reason for the (Ms-Mw)>0.2 in the inland earthquake is that the earthquakes occur on the faults of more complicated structure than the

faults at the plate boundary. In order to draw a conclusion, it is necessary to know the structure of a fault, especially around its tips.

Keywords: fracture energy, seismic efficiency, magnitude, moment magnitude, damage zone fault model , critical weakening displacement

Early recurrence of M~6 intraplate earthquake (5.8 years) observed in northern Kanto region, Japan

*Yo Fukushima[1], Shinji Toda[1], Satoshi Miura[2]

1. International Research Institute of Disaster Science, Tohoku University, 2. Graduate School of Science, Tohoku University

On 28 December 2016, an M~6 normal fault earthquake occurred in the northern part of Ibaraki prefecture in Kanto region, Japan (hereafter called event B). This event was observed by the Japanese ALOS-2 satellite equipped with PALSAR-2, an L-band synthetic aperture radar (SAR). Interferometric SAR (InSAR) processing indicates clear displacement discontinuity line, directing approximately NW-SE. The amount of discontinuity is ~30cm in the line-of-sight (LOS) direction (approximately from East with incidence angle of 36 degrees). A preliminary inversion found a dip angle of 42 degrees with fault slip confined in the upper-most 5km in the crust.

The region has experienced swarm-like normal faulting activities after the occurrence of the 11 March 2011 Mw9.0 Tohoku-oki earthquake including an Mw6.6 event composed of complex ruptures on multiple faults (e.g., Fukushima et al., 2013, BSSA). One of such events was an M~6 event on 19 March 2011 (hereafter called event A).

We performed InSAR analysis also for the event A using the data acquired by the ALOS satellite equipped with PALSAR radar. After removing the displacements caused by the Tohoku-oki earthquake, we obtained a remarkably similar displacement pattern for the event A as compared with the event B. Specifically, the locations of displacement discontinuity lines were almost identical, and the amount of displacement discontinuity was up to ~45cm for the event A and ~30cm for the event B. The displacement patters were similar, both indicating southwestward normal faulting on a NW-SE striking fault, suggesting that the same fault ruptured. The slight larger displacement for event A indicates that this event was associated with slightly larger slip on the fault at least close to the ground. The InSAR data for the event A presumably includes the displacements associated with an Mj 5.7 event, which should be taken into account for further comparison.

Our result indicates that the same M~6 fault can re-rupture in a very short time interval of 5.8 years. Two interpretations are possible as to the mechanism of the extremely early recurrence: 1) rapid loading of the fault occurred after the event A, possibly associated with the postseismic deformation due to the 2011 Tohoku-oki earthquake, and 2) stress level on the fault remained high after the event A, enabling further slip on the fault, without significant loading.

Keywords: InSAR, crustal deformation, earthquake recurrence, intraplate earthquake

Development of trans-dimensional source inversion with geodetic data

*Hisahiko Kubo[1], Wataru Suzuki[1], Akemi Noda[1], Shin Aoi[1]

1. National Research Institute for Earth Science and Disaster Prevention

In this study, we develop a new approach to estimate the static slip distribution from geodetic data by the trans-dimensional inversion, which estimates the dimension of model parameters as well as values of model parameters. The trans-dimensional inversion has been recently applied in the geophysical field (e.g. Agostinetti and Malinverno 2010; Bodin et al. 2012; Hawkins and Sambridge 2015; Kubo et al. 2016 JpGU) including the source inversion (e.g. Dettmer 2014). An advantage of this approach on the source inversion is that it does not require the smoothing constraint on slips as the prior information. The smoothing constraint is widely used in the source inversion to obtain stable and physically reasonable solutions; however, the use of the smoothing constraint significantly reduces the resolution of the source inversion. In the case of the biased and/or sparse station distribution, the source inversion with this constraint is likely to produce the solution largely affected by the prior information. Another advantage is that the posterior distributions of model parameters directly produced by sampling methods such as Markov chain Monte Carlo (MCMC) method are useful for the estimation of model uncertainties.
We assume the linear observation equation: the static slips on fault are linearly related to the static displacement at receivers via Green’ s functions. For simplicity, the errors of the observation equation are assumed to follow a Gaussian distribution and to be independent of each other. We model the static slip distribution on fault by a variable number of Voronoi cells. Unknown parameters are the number of Voronoi cells, the locations of Voronoi cells on fault, and slip values of Voronoi cells. We impose the non-negative constraint on this inverse problem following the procedure of Fukuda and Johnson (2008) and Kubo et al. (2016 GJI). To obtain the distribution of the model parameters, we employ the reversible jump MCMC method (Green 1995), which selects the action in each sampling step from four candidates: birth of Voronoi cell, death of Voronoi cell, move of Voronoi cell, and slip change of Voronoi cell. To improve the efficiency of the probabilistic sampling and the search range of parameter spaces, we use the parallel tempering algorithm (e.g. Sambridge 2013) in the ensemble sampling. For Green’ s functions, we calculate the theoretical static displacements caused by a unit slip on each subfault assuming a homogeneous elastic half-space (Okada 1992).
We apply this newly-developed approach to real GNSS data of the 2015 Gorkha, Nepal, earthquake (Galetzka et al. 2015; Kubo et al. 2016 EPS). Because the station distribution is sparse in this event, the GNSS data are expected to have a limited resolution of fault slips. We found that the conventional source inversion with the smoothing constraint produces the unsharp slip distribution where slips are widely distributed over the assumed fault. On the other hand, our new approach produces the sharp slip distribution that has large slips north of Kathmandu and no slip at the other places. The data fit of this approach is better than that of the conventional approach. This result demonstrates that the introduction of the trans-dimensional approach to the source inversion leads to the acquisition of the source model composed of only meaningful slips that are necessary to explain the data. The estimated posterior distributions in the large slip region suggest that the variation of slips is small in the area surrounded by several stations and large in the area far from stations, which is consistent with our intuitive understanding of the source process inversion.

Keywords: Source inversion, Trans-dimensional inversion, Geodetic data

Potency Backprojection

*Ryo Okuwaki[1], Amato Kasahara[1], Yuji Yagi[2]

1. Graduate School of Life and Environmental Sciences, University of Tsukuba, 2. Faculty of Life and Environmental Sciences, University of Tsukuba

The backprojection (BP) method has been used as a tool to image the rupture propagations of the M8–9 megathrust earthquakes since its successful application to the Mw 9.1 2004 Sumatra-Andaman earthquake. The BP method back-projects waveforms onto a point of a source area by stacking them with theoretical travel time shifts between the point and the stations. The hybrid backprojection (HBP) method, an alternative BP technique, resolves a spatiotemporal distribution of waveform-radiation sources by stacking cross-correlation functions of the observed waveforms and theoretically calculated Green’s functions. As the Green’s function contains information of the direct P-phase as well as the later phases (pP and sP phases), the HBP method enhances the depth-resolution of the image and mitigates the dummy-imaging of the later phases, which had been the shortcomings of the conventional BP method. Both methods are able to track high-frequency (HF) radiation sources, which are hard to be resolved with the waveform inversion method. The HF waves are radiated when rupture velocity and/or slip rate abruptly change, and contain rich information of a heterogeneous rupture evolution. Thus, an integrated analysis with the BP/HBP method and the waveform inversion provides us fruitful information to understand the rupture process of a megathrust/large earthquake.

The intensity at a point of the BP/HBP image represents how much wave radiated from the point accounts for the observed waveforms. Since the amplitude of the Green’s function associated with unit slip-rate increases with depth as the rigidity increases with depth, the intensity of the BP/HBP image inherently has a depth dependence. To make a direct comparison of the BP/HBP image with a slip distribution inferred from the waveform inversion, and discuss the rupture properties of the fault, it should be required the BP/HBP image to represent the slip-rate distribution that corresponds to the potency rate density distribution.

Here we propose new formulations of the BP/HBP methods, which image the potency rate density distribution by refining the normalizing factors in the conventional formulations. For the BP method, the observed waveform, that is shifted with the relative travel time, is normalized with the maximum amplitude of P-phase of the theoretically calculated Green’s function. For the HBP method, we normalize the cross-correlation function of the observed waveform and the Green’s function with the squared-sum of the Green’s function. The normalized waveforms and the cross-correlation functions are then stacked for all the stations to enhance the signal to noise ratio, and the back-projected image now represents the potency rate density distribution.

We tested the new formulations against synthetic waveforms and the real data of the Mw 8.3 2015 Illapel Chile earthquake. We back-projected the synthetic waveforms originated from randomly distributed synthetic source points possessing a uniform potency. The resulting image intensity at the shallow parts of the fault was increased compared to that from the conventional formulations, reproducing the potency distribution of the input model. The intensity, however, were still weak at the very shallow parts, where the relative travel time between the P-phase and the later phases are very close. We also applied the new formulations to the real data, and found that the intensity of the image at shallower than 25 km depth was also slightly increased, compared to that from the conventional formulations.

Keywords: Backprojection, Imaging of rupture evolution, Depth dependence, Seismic source process, Potency

Analysis of seismic source process during the 2016 Kumamoto earthquake by jointly using surface ruptures and teleseismic waveforms

*Keita Kayano[1], Yuji Yagi[1]

1. Tsukuba University

Waveform iversion of teleseismic body waves has been applied to earthquakes to analyze an earthquake source process. However, it is difficult to resolve fault slip near the surface because the relative travel time between the direct P-wave and the reflected waves becomes short and the waveform signal generated by a near-surface slip becomes small with increasing of the slip duration. On the other hand, we can measure relative displacement along surface ruptures with high accuracy after an occurance of the earthquake. By jointly using the teleseismic waveforms and the surface rupture observations, it is possible to estimate a source process of an earthquake, even for the past earthquakes which we do not have enough data with recent developed techniques such as InSAR or GPS. In this study, we demonstrated the utility of the joint inversion of teleseismic data and field survey data through analysis of the 2016 Kumamoto, Japan earthquake (M_{JMA} 7.3).

We used vertical components of teleseismic P body waves observed at 27 stations of the Global Seismographic Network (GSN) and relative displacements of surface ruptures at 408 measurement points (Kumahara et al. 2016, JpGU). It is difficult to uniquely determine variance of the field survey data since measurement errors of the data depend on the appearance-clarity of each measurement object (e.g., water channels, furrows on rice fields). We determined the relative weights among the teleseismic body waves data, the field survey data, and prior information using the Akaike’ s Bayesian information criterion (ABIC). We assumed a planar single fault model (strike: 234˚, dip: 64.0˚) along the Hinagu-Futagawa fault zone based on the focal mechanism, aftershocks distribution, and the surface ruptures. To describe in detail a slip behavior around a junction of the two fault zones, we discretized the fault model into 2 km ×2 km sub-faults and deployed 49 B-spline functions expressing source time functions of each sub-fault at intervals of 0.3 s. We projected the field survey data to the uppermost sub-faults on the fault model.

Main rupture can be seen in the Hinagu fault area from rupture initiation to 8 s where a right-lateral slip is dominant. The rupture then shifts to the Futagawa fault area, and gradually propagates to the surface with a right lateral slip involving normal faulting. The rupture terminates southeast side of Mt. Aso caldera at about 15 s after rupture initiation. From the total slip distribution, we can see a maximum slip of around 3 m along the Futagawa fault area, and a right lateral motion is dominant along the entire Hinagu fault area, while a right lateral slip with a normal faulting prevails along the entire Futagawa fault area.

Comparing the result with one estimated by using only the teleseismic body waves, we can see clear differences in spatiotemporal distributions of slip-rate near the surface. In the result from only the teleseismic records, the slip at the shallower than 1 km depth occurs at 7 s after rupture initiation and continually occurs along both the Hinagu and Futagawa fault areas until 15 s. In the result of the joint inversion, however, the time of occurrence of the slip is about 10 s after initiation, which is later than that by solely using teleseismic body waves. Synthetic waveforms of both the joint analysis and the teleseismic analysis well capture the characteristics of the observed waveforms, while the total slip and the slip directions near the surface estimated by the joint analysis are more consistent with the surface ruptures, compared with those from the teleseismic analysis. The path of the rupture propagation, the rupture transition from the Hinagu fault to the Futagawa fault, and the spatial pattern and the depth of maximum slip are consistent with the results from the strong motion records based on the detail fault geometry and

the InSAR data. The result in this study suggests that we can acquire the detailed slip distribution even if we use a simple planar fault model by using the field survey data together with the teleseismic body waves.

Keywords: Joint inversion using ABIC, Field survey data, 2016 Kumamoto earthquake

3D seismic velocity structure in the lower crust beneath the San-in district

*Hiroo Tsuda[1], Yoshihisa Iio[2], Takuo Shibutani[2]

1. Graduate School of Science, Kyoto University, 2. Disaster Prevention Research Institute, Kyoto University

Introduction

In the San-in district, a linear distribution of epicenters is seen along the Japan Sea coast. The linear distribution of epicenters is called the seismic belt along the Japan Sea coast. Large earthquakes also occurred in and around the seismic belt. What localizes the distribution of earthquakes in the San-in district far from the plate boundary? We thought that we could explain the reason by the model proposed by Iio et al. (2002, 2004). The model is as follows. A part of the lower crust has low viscosity. The low viscous part was called 'weak zone'. The stress and strain in the upper crust are concentrated right above the weak zone and earthquakes occur there. We estimated the seismic velocity structure in the lower crust beneath the San-in district in detail by carrying out seismic travel time tomography to verify whether the weak zone exists there.

Seismic travel time tomography

We carried out the tomography with FMTOMO (Rawlinson et al., 2006). FMTOMO implements wavefront tracking (de Kool et al., 2006), which can trace rays robustly. We set the study area shown in Figure 1. We used travel times picked by JMA for earthquakes that occurred in the study area (Figure 1), as well as with the travel times manually picked for earthquakes that occurred within the Philippine Sea Slab (PHS). Because seismic waves from these earthquakes to stations in the San-in district pass through the lower crust beneath the San-in district, we can expect that those data improve the resolution at the lower crust. Because those seismic waves also pass through the PHS, the velocity structure in and around the PHS plays an important role in this study. However, the dataset used in this study is not enough to estimate accurately the velocity structure. For this reason, we estimated in advance rough velocity structure in a wider area shown in Figure 2, and used the velocity structure as an initial velocity model.
In this study, we revealed that the lower crust beneath the seismic belt in the San-in district has low velocity anomalies. Since velocities of rocks decrease with temperature or fluid content, the lower crust beneath the San-in district might have low viscosity (weak zone). Therefore, the results of this study support the model proposed by Iio et al. (2002, 2004).

Acknowledgement: We used JMA's earthquake catalogs. We also used waveform data from permanent stations of NIED.

Keywords: tomography, San-in district, lower crust, intraplate earthquake

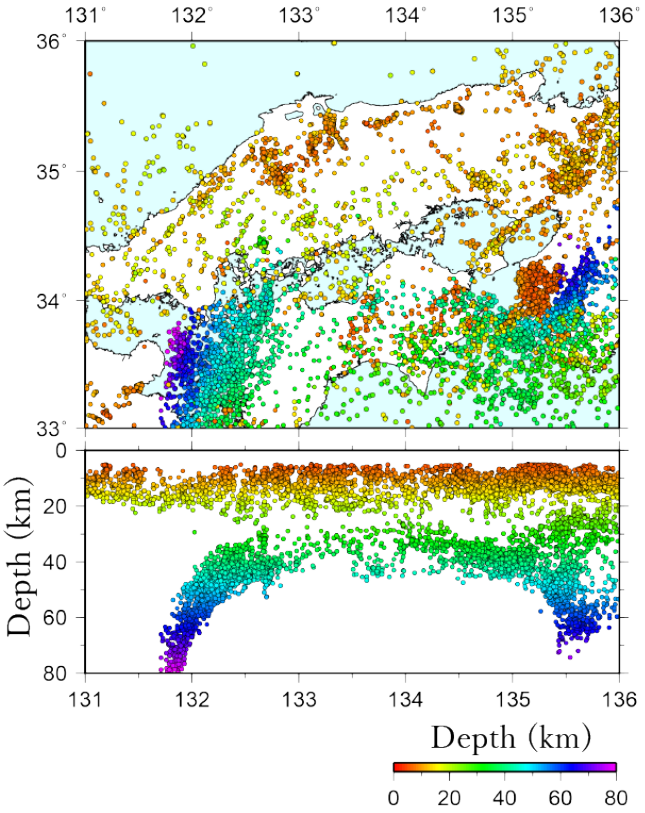

Figure 1 The distribution of earthquakes used in the tomography.

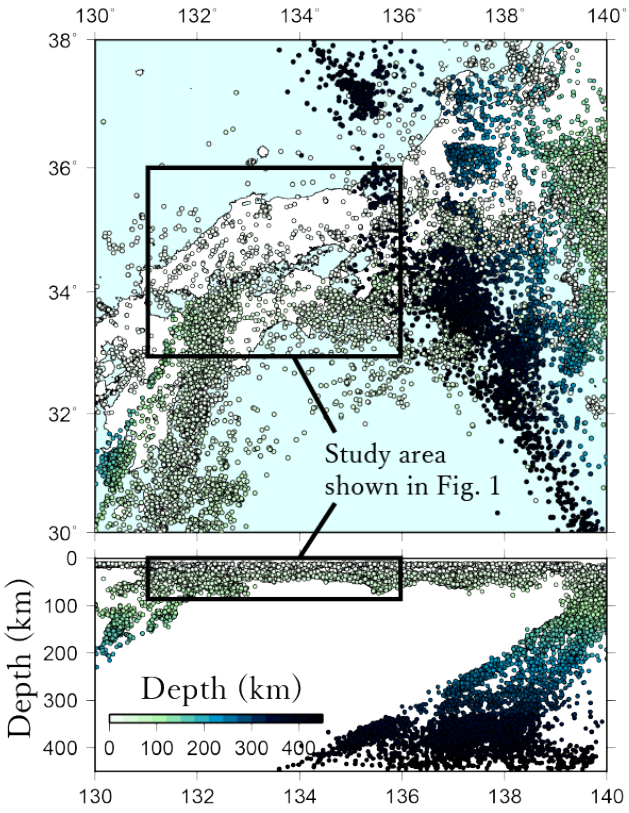

Figure 2 The distribution of earthquakes used for estimating rough velocity structure of an wide region which is used as an initial velocity model.

Swarm activity beneath Sendai-Okura Dam, NE Japan, induced by the 2011 Tohoku-Oki earthquake - Precise hypocenter distribution and fine fault structure

*Keisuke Yoshida[1], Akira Hasegawa[1]

1. Tohoku University

An earthquakes occurs when shear stress acting on a weak plane reaches its frictional strength. Therefore, we can roughly divide the cause of earthquake occurrence into two: increase in shear stress and reduction in frictional strength.
There occurred several earthquake swarms in NE Japan induced by the 2011 Tohoku-Oki earthquake, regardless of the reduction in ΔCFF. Since they commonly show the migration behavior of hypocenters as well as the delay of the their initiation of a few days to a few weeks after the Tohoku-Oki earthquake, several studies suggested that these swarms were caused by the reduction in frictional strength due to the increase in pore pressure by fluids rising from below [Yoshida et al., 2012; Terakawa et al., 2013; Okada et al., 2015; Yoshida et al., 2016].
In order to know detailed behavior of crustal fluids, we investigated spatio-temporal distribution of hypocenters in an earthquake swarm beneath Sendai-Ohkura Dam that was induced by the Tohoku-Oki earthquake. Approximately 10 km southeast of this swarm, an M5.0 earthquake took place in 1998. Subsequent studies showed that there exist a remarkable S-wave reflector in the middle crust [Umino et al., 2002]and a prominent low-velocity zone in the lower crust right beneath the source area [Nakajima et al., 2006].
Spatial distribution of earthquake hypocenters listed in JMA catalogue shows a slightly east-dipping cloud-like distribution with ~4km width, probably due to the errors in hypocenter locations, which makes it difficult to understand the detail of hypocenter migration. We relocated hypocenters by using the cross-correlation of waveforms to obtain a clearer image of hypocenter migration.
First, we classified earthquakes based on waveform similarity. When there is an event pair with correlation coefficient >0.92 at least at three stations within 20 km from the swarm region, we regarded them as similar earthquakes. We then searched for other similar events. Repeating the same procedure, we produced groups of similar events. As a result, we obtained 7 similar earthquake groups involving >30 events.
Second, we computed cross correlations of P- and S-waves of the event pairs with their epicenter separations less than 2 km, and obtained normalized cross correlation coefficients and differential times. By using differential times with normalized cross correlation coefficient higher than 0.9, scatter of S-P times reduced from 0.2s to less than 0.05s. By adding the differential time data thus obtained to the manually picked arrival time data, we relocated hypocenters by the Double-Difference method [Waldhauser & Ellsworth 2002]. The residuals of differential time reduced from ~120 ms to ~10 ms after 30 times iteration.
Hypocenter distribution drastically changed from the original east-dipping cloud-like scatter to the distribution on several sharp planes. Similar earthquakes in one group concentrate on a common fault plane. Most of the hypocenter alignments are dipping to the west. However, there exist some subhorizontal alignments. Their focal mechanisms are consistent with this alignments, which are unfavorably-oriented from the regional stress field. This suggests that the strength of fault planes decreased as suggested from the hypocenter migration. The relocated distribution of hypocenters shows that the hypocenters migrated along the fault planes mainly from deeper to shallower parts.

Keywords: crustal fluid, frictional strength, 2011 Tohoku-Oki earthquake, swarm

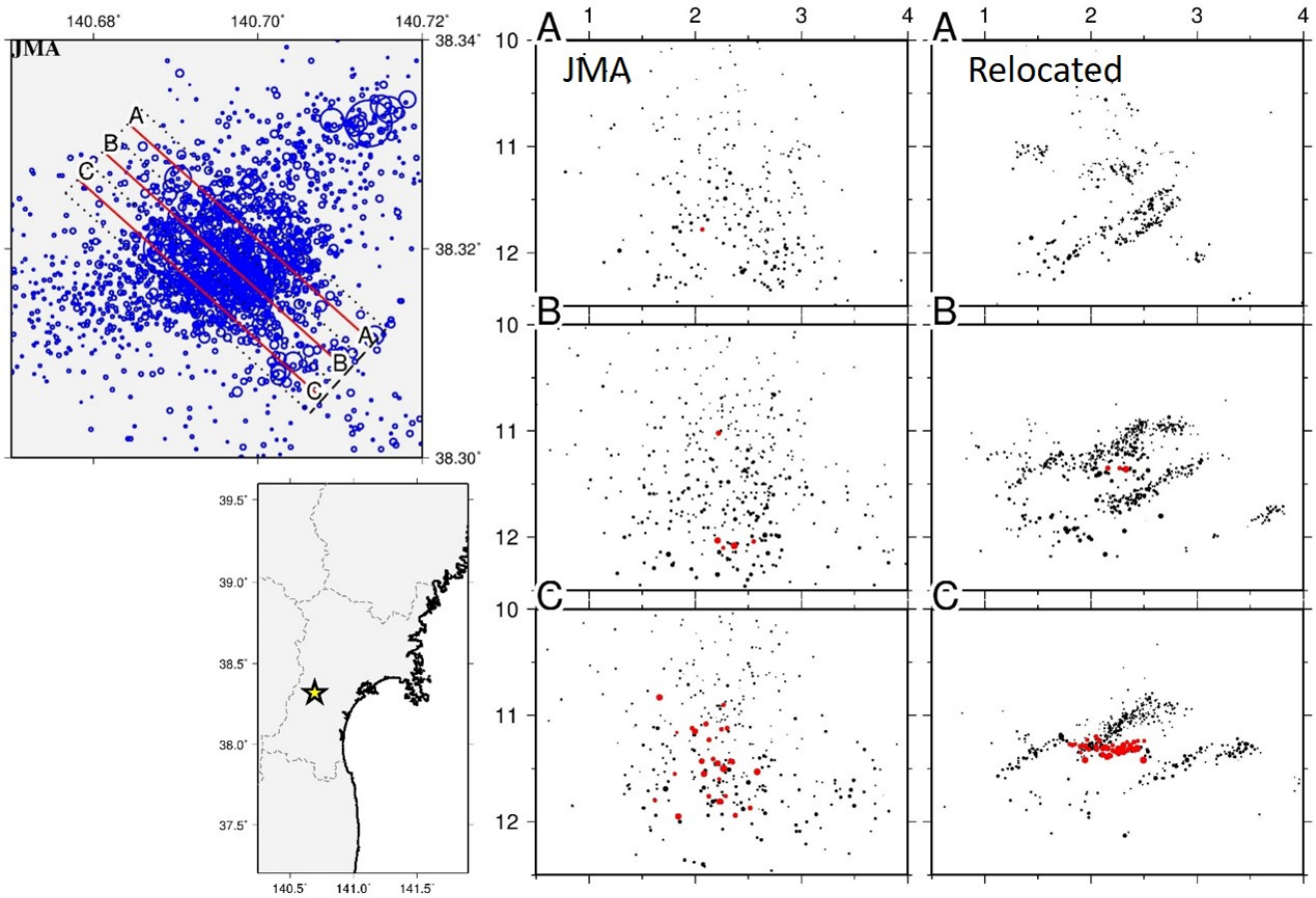

Record of slow slip instabilities in rocks: the role of silica redistribution in the behavior of subduction interfaces

*Donald M Fisher[1], Andrew Smye[1], Chris Marone[1], Asuka Yamaguchi[2]

1. Department of Geosciences, Penn State University, 2. Atmosphere and Ocean Research Institute, The University of Tokyo

We present observations from nine regional fault zones exposed in the ancient, sediment-dominated Kodiak and Shimanto accretionary complexes. There are characteristics common to all these examples that suggest a record of slow slip instabilities that deform the underthrusting footwall at a range of depths within and around the seismogenic zone. These fault zones, in some cases 10’s of m’s thick, have a block-and-matrix fabric but are structurally systematic, with evidence for a compactive strain path and simple shear along a web-like array of scaly slip surfaces in fine-grained lithologies. These slip-related microstructures are coincident with silica redistribution, with silica depletion along slip surfaces and precipitation of quartz and other silicates in veins within coarser clasts and along extensional jogs in slip surfaces.

The fault rocks contain several features that suggest a record of slow slip and quasi-dynamic fault motion: 1) scaly shears represent locations of diffusive mass transfer, suggesting linear viscous flow, a rheology favored by low strain rates, 2) there is clear evidence for repeated antitaxial and syntaxial cracking and sealing, in some examples directly related to slip on shear surfaces—an observation that is consistent with slip instabilities as it requires cyclic behavior rather than continuous creep, 3) the zone of deformation is wide, indicative of distributed shearing on many slip surfaces, with large slip distances and a strain hardening process on individual features, and 4) small (10’s of microns) magnitudes of slip during cracking and slip.

We propose a conceptual model for propagating, slow ruptures that move at rates dictated by shear processes within a zone of finite thickness. The fault rocks suggest that stress rises at the propagating front of a slow slip instability, leading to quasi-plastic failure in the form of scaly slip surfaces in the footwall. Development of slip surfaces represents a weakening mechanism due to loss of cohesion or alignment of phyllosilicates, but each slip surface subsequently hardens because of increases in normal stress associated with hydrofracturing or by the activation of a hardening mechanism such as pressure solution and ensuing reduction in fracture porosity. Thus, the development of a distributed scaly foliation and vein system leads to initial softening but has an inherent stabilization mechanism for putting on the breaks and keeping things slow.

Based on these observations, we construct a kinetic model to estimate the time required to seal fractures. This model accounts for the interplay between spatial gradients in chemical potential and pressure within a vein-rock system. Vein sealing is driven by diffusive redistribution of Si from solid-solid surfaces to undersaturated veins. The model predicts that healing of cracks in subduction zones occurs on secular time scales. Temperature exerts a primary control on healing rate and variations in the temperature structure of different convergent margins leads to a wide variability in sealing times. Correlation between plate age and the b-value of earthquake size distributions could reflect temperature through the kinetics of reactions and the healing rates of fractures. The evidence from ancient rocks for stress cycling, repeated fracturing, and thermally activated crack healing in underthrusting sediments could play an important role in modulating the behavior of the footwall of the subduction interface, and the spatial roughness in this behavior for different subduction zones could be an important control on seismicity.

Keywords: Slow slip, silica kinetics, earthquakes

Constraining the thickness of tremor source region on the basis of seismological and geological observations in southwest Japan

*Kazuaki Ohta[1], Yoshihiro Ito[1], Kohtaro Ujiie[2], Ake Fagereng[3], Satoshi Katakami[1], Takahiro Kinoshita[2]

1. Disaster Prevention Research Institute, Kyoto University, 2. University of Tsukuba, 3. Cardiff University

Recent studies have shown that slow earthquakes such as tremors and slow slips along subduction zones are shear slips on the plate interface of subducting oceanic slab (e.g. Ide et al., 2007). Although the seismologically determined depth range of tremors is several km and still has large uncertainties, such tremor zone is usually treated as a flat fault plane with no thickness. On the other hands, the recent geological observation has discovered the records of past tremors and suggested that tremors occur in the deformation zone with the thickness of tens of meters (Ujiie et al., 2016, AGU Fall Meeting). Here we try to reconcile these two observations by estimating the thickness of the tremor zone based on both the seismological and geological approaches.

For the seismological approach, we focus on the thickness of the hypocenter distribution of tremors in Shikoku region, southwest Japan. As representatives of tremor sources, we use the deep low frequency earthquakes (LFEs). By applying the NCC hypocenter determination method (Ohta and Ide, 2011) based on the summed cross-correlation coefficients across the network (NCC) to Hi-net velocity seismograms, we accurately relocate 2450 LFEs in the catalog of Japan Meteorological Agency from 2004 to 2011. Relocated hypocenters of LFEs are highly concentrated in the depth direction and show gradual inclinations consistent to the geometry of the oceanic Moho of the subducting Philippine Sea Slab (Shiomi et al., 2008). We fit a polynomial surface to the distribution for each cluster by minimizing the vertical offsets in the least-squares sense and measure the thickness as their deviation. The thickness of each cluster ranges from ~50 m to ~1700 m.

For the geological approach, we examine the vein distribution in the Makimine tectonic mélange in the Shimanto accretionary complex in southwest Japan. The mélange is considered to be shear zone along subducting plate and preserve numerous shear veins accompanied by extension veins. We regard the shear vein concentration zone as the tremor zone and measure its thickness along the transect perpendicular to the foliation. We further examine the number and length distribution of the veins. Within the entire exposure of ~120 m thickness, shear veins are concentrated in the zone of ~60 m thickness. We observed numerous shear veins as well as foliation parallel extension veins. The number of veins along the transect is 1147 in total. The lengths of the shear veins are from 1 to 7 m and most are around 1 m.

The geologically determined thickness (60 m) of the tremor zone is within the range of the seismologically determined thickness (50-1700 m), which supports the idea that the observed shear veins are the faults of tremors. The lengths of veins (~1 m) are much smaller than the fault size of tremor and other slow earthquakes (>100 m). However, a cascading failure of the faults caused by the entire zone deformation can possibly produce larger events. The coexistence of the shear veins and foliation parallel extension veins indicates high pore pressure in the tremor zone that exceeds the least stress. We further expect extension components associated with extension veins in the focal mechanism of slow earthquakes.

Keywords: tremor, low frequency earthquake, Makimine tectonic mélange, subduction zone

Microscopic derivation of rate- and state-dependent friction and its scaling properties

*Takahiro Hatano[1]

1. Earthquake Research Institute, University of Tokyo

In this talk, a scaling argument is given for the the length constant in the rate- and state-dependent friction law.
In general, the dynamic friction coefficient is not the single-variable function of the sliding velocity, as friction involves some aging processes such as frictional healing. Therefore, one needs additional variables to describe the behavior of friction coefficient. In the simpleset case, a single “state variable” is introduced to describe an aging process and the friction coefficient is described with the two variables: the sliding velocity and the state variable. This formulation is referred to as the rate- and state-dependent friction (RSF) law. It includes three important parameters and they determine the frictional stability/instability. Thus, it is widely used to understand earthquakes as the frictional instability. Unfortunately, to this date, the RSF is purely empirical and therefore one cannot judge its applicable limit. In addition, it is not clear at all how these important parameters are determined from (or related to) the physical entity of the fault surface.
Because the macroscopic friction force is supported by microscopic junctions of protrusions, any macroscopic friction law should be derived from constitutive laws of such microscopic junctions. With this procedure one can overview the micro-macro correspondence in friction and understand the physical meaning of phenomenological parameters in an macroscopic friction law. Here we carry out this program for the RSF law; i.e., we derive the RSF from constitutive laws of the microscopic junctions. Consequently, the microscopic expressions are given of the RSF parameters such as the relaxation length Dc. The system-size dependence of the relaxation length is discussed.

Keywords: friction law, critical slip distance

Deformation experiment on quartz aggregates with high water contents at high pressure and temperature

*Keishi Okazaki[1,2], Greg Hirth[2]

1. Japan Agency for Marine-Earth Science and Technology, 2. Brown University

Large earthquakes typically nucleate near the depth limit of seismogenic zones. In these areas, high V_p/V_s ratios are commonly observed, indicating the presence of high pore fluid pressures. Thus, it is important to understand how the water content (both water in the crystal and in the pores) and the pore structure affect the rheology of polycrystalline materials.
We conducted deformation experiments on quartz aggregates using a Griggs-type deformation apparatus. Samples were hot-pressed from silica gels, which contain ~9 weight percent water within the amorphous structure and absorbed on the surface. Hydrostatic experiments within the alpha-quartz stability field at a pressure of 1.5 GPa and 900oC indicate that hot-pressed samples are composed of quartz and no relict of amorphous material is present. The average grain size and porosity of the hot-pressed aggregates is about 6 um and 0.23, respectively. The grain shape is equigranular and no crystallographic preferred orientation (CPO) is observed.
Initial results from general shear experiments on the hot-pressed quartz aggregates at the equivalent strain rate of 1.5×10^{-4} 1/s, a pressure of 1.5 GPa and 900°C show very low strength (equivalent stress of 140 MPa) and nominally steady state flow at shear strains up to 3.5. The samples show weak CPO; a-axis of quartz aligned parallel to the P direction. We also found an evidence for strain localization along R_1 riedel shears, which structure is characterized by high porosity zones. In contrast, deformation experiments on cores of quartzite show dislocation creep at this pressure/temperature condition.
The stress exponent *n* is 2.8–3.4 indicating that the dislocation creep of quartz presumably controls the overall rate-behavior in the quartz shear zone. The measured stress from the new experiments is significantly lower than predicted by the wet quartz flow law (e.g., Hirth et al., 2001). The low flow stress and R1 reidel shear zones suggest that the stress enhancement process (Hirth and Kohlstedt, 1995) is activated by the high volume amount of water or perhaps the effective pressure law is still applicable and the sample deforms by a semi-brittle flow process.

Keywords: brittle-ductile transition, strain localization, earthquake

Determination of the deformation conditions of the shear zone using fault rocks: an example for the Asuke Shear Zone

*Takuto Kanai[1]

1. Graduate school of creative science and engineering, Waseda University

The Asuke Shear Zone (ASZ) transects the Inagawa Granodiorite in the Ryoke Belt, and it extends NE–SW for ~14 km and is several tens to hundreds of meters wide around Asuke Town, Aichi Prefecture. Cataclasites constitute entirely the ASZ, whereas pseudotachylytes and mylonites are also observed in the central segment of about 4.5 km along the ASZ (Sakamaki et al., 2006). The ASZ is considered to be deformed in cataclastic-plastic transition regime of granitic crust (Sakamaki et al., 2006). Kinematic indicators and stretching lineations in the mylonites indicate a sinistral–normal shear. In this presentation, I will summarize (1) the paleostress orientations during the formation of mylonite using slip data of the shear zone and healed miocrocracks in quartz grains in the protolith granite, and (2) those just after the formation of pseudotachylyte using microstructure of calcite infilling amygdales. I will also summarize the deformation conditions of the ASZ using microstructures of recrystallized quartz grains and those of calcite grains.

In the high strain area such as the central part of the shear zone, it is believed that the mylonitic lineation defined by the stretching lineation is parallel to the displacement direction of the shear zone (Simpson, 1986). Assuming that the Wallace-Bott hypothesis that the displacement direction is parallel to the direction of the shear stress acting on the slip surface, the combination of the mylonitic foliation and lineation of mylonite which can judge the shear sense can be used for paleostress analysis as well as fault slip data. The mylonites strike NE–SW to ENE–WSW and dip 50–70˚ to the N, and mylonitic lineations plunge 40-50˚ to the NW. As a result of the Hough-transform-based inversion method (Yamaji et al., 2006), the optimum estimated σ_1 axis trends 183˚ and plunges 63˚, whereas the σ_3 axis trends 310˚ and plunges 14˚. The stress ratio is 0.56. Kanai and Takagi (2016) reported the Z-maximum quartz *c*-axis LPO patterns from the mylonitized pseudotachylyte that was used for the paleostress analysis this time, and the deformation temperature was estimated of 300-400 ˚C. Moreover, differential stress is estimated to have been 110–130 MPa based on the recrystallized grain size.

Paleostress orientation analysis using calcite *e*-twins in the amygdales of the pseudotachylytes has been carried out (Kanai and Takagi, 2016). The optimal estimated σ_1 axis trends 228˚ and plunges 55˚, whereas the σ_3 axis trends 320˚ and plunges 1˚. The stress ratio is 0.78. The deformation temperature and differential stress estimated by the morphology of the *e*-twins (Burkhard, 1993) and the twinning ratio (Yamaji, 2015) give 150-200 ˚C and 40-80 MPa, respectively. The misfit angle of the stress tensor estimated from the mylonite and the calcite *e*-twin is 23.1˚. Although deformation temperature, differential stress and deformation scale are different in recrystallized quartz in mylonite and calcite amygdales in pseudotachylyte, the principal stress axes orientation estimated from mylonite and calcite are similar. The timing of mylonitization and calcite twinning is about 70 and 50 Ma, respectively, on the basis of the deformation temperature of mylonites, cooling curve of the Inagawa Granodiorite (Yamasaki, 2013) and fission-track zircon age of pseudotachylyte (Murakami et al., 2006). The ASZ is considered to have been activated under the single paleostress filed that involves the orientation of NW-SE subhorizontal $\sigma 3$ axis and $\sigma 1$ axis plunging 60˚ S~SSW during 70-50 Ma.

References

Burkhard, M., 1993, *Jour. Struct. Geol.*, **15**, 351-368.
Kanai, T. and Takagi, H., 2016, *Jour. Struct. Geol.*, **85**, 154-167.

Murakami, M., Kosler, J., Takagi, H. and Tagami, T., 2006, *Tectonophysics*, **424**, 99-107.
Sakamaki, H., Shimada, K. and Takagi, H., 2006, *Jour. Geol. Soc. Japan.*, **112**, 519-530.
Yamaji, A., 2015, *Jour. Struct. Geol.*, **72**, 83-95.
Yamaji, A., Otsubo, M. and Sato, K., 2006, *Jour. Struct. Geol.*, **28**, 980-990.
Yamasaki, T., 2013, *Jour. Geol. Soc. Japan.*, **119**, 421-431.

Keywords: Asuke Shear Zone, mylonite, paleostress analysis

Seismic and tsunami waveform analyses for the 1938 and 2016 Off Fukushima earthquake sequence

*Satoko Murotani[1], Kenji Satake[2]

1. National Museum of Nature and Science, 2. Earthquake Research Institute, University of Tokyo

The 1938 Off Fukushima (Shioya-oki) earthquake sequence, which consists of five earthquakes of M_{JMA} ranging from 6.9 to 7.5, occurred in the southern part of the 2011 Tohoku earthquake source area. In this region, a normal fault earthquake occurred on November 22, 2016 (M_w 6.9) . To understand their source processes, we re-examined seismic and tsunami waveform records. Murotani et al. (2004, SSJ Fall Meeting) estimated slip distributions for event 1 on May 23 (M_w 7.6, Fault size 60 km x 70 km), event 2 on November 5 (M_w 7.9, Fault size 80 km x 60 km), and event 3 on November 5 (M_w 7.8, Fault size 90 km x 60 km) from inversion analyses of near field seismic waveforms at Sendai, Niigata, Maebashi, Mito, and Hongo (Tokyo). In this study, we compared the observed teleseismic waveforms at Christchurch (CHR), De Bilt (DBN), Pasadena (PAS), and Pulkovo (PUL) with the calculated waveforms from the above slip distributions. The result showed that the amplitudes of computed waveforms for all events were several to several tens of times larger than the observations. We also calculated the tsunami waveforms using the slip distribution for Event 2, and compared with the observations at Hachinohe, Ayukawa, Miyako, Ojima, and Onahama. The amplitudes of calculated tsunami waveforms were also larger than the observations. These indicate that the slip amount and M_w obtained from the near field seismic waveforms inversion were over-estimated. Then, we compared the normal fault event of 1938 (event 4 on November 6) with the 2016 (M_w 6.9) event. Although there were only a few tsunami records from the same stations, the waveforms are not similar. The teleseismic waveforms of event 4 is similar to those of 2016 event. The re-analyses of near field seismic data using the heterogeneous velocity model will be also presented in the presentation.
This study was supported by JSPS KAKENHI Grant Number JP16H01838.

Keywords: 1938 and 2016 Off Fukushima earthquake, Source process, seismic and tsunami waveforms

Fault Slip Distribution determined by Automated Source Process Analysis with Teleseismic Body-Wave based on Scaling Relationships Derived from Fault Slip Distributions

*Kenichi Fujita[1], Akio Katsumata[1], Iwakiri Kazuhiro[2], Miho Tanaka[2]

1. Meteorological Research Institute, 2. Japan Meteorological Agency

1. Introduction

We have examined optimized preset parameters for automatic source process analysis with teleseismic body-wave. First, we set size of fault and subfault based on scaling relationships derived from fault slip distribution studies, and we investigated that fault plane included rupture area for many events. Then, we set sampling rate and rise time of basis function based on subfault size, and we investigated that we could avoid instability of the solution caused by setting too high-resolution temporal or spatial parameters for many events. Finally, we set other parameters by using experiential knowledge, and we investigated that we could set all parameters for automatic source process analysis based on hypocenter data and focal mechanism data.

This time, we set parameters more precisely based on event magnitude, we selected stations automatically by using signal-to-noise ratio of waveforms, and pick P-wave onset time automatically by using an auto-pick program for hypocenter determination. Thus we have become to do source process analysis automatically.

In this report, we investigated fault slip distributions of large earthquakes (M7.5) determined by automated source process analysis. And for verification, we compared fault slip distributions and aftershock distributions, and others.

2. Analysis Methods

We used the same program package as Iwakiri et al. [2014] for analyzing source process with teleseismic body-wave. This program package is modification of the program package by Kikuchi and Kanamori [2003]. We used broadband waveform data which were downloaded from IRIS DMC HP, and set sampling rate and band-pass filter band based on event magnitude. We used hypocenter data of JMA for events in and around Japan, and USGS for events in other areas. We used focal mechanism data of JMA for events in and around Japan, and W-phase moment tensor of USGS for events in other areas. Hypocenter was assumed as the center of fault plane, and subfault size was set based on event magnitude (number of subfault were fixed). Source-time function was set as triangle functions, and rise time was set based on event magnitude (number of basis function were fixed). Preset source time duration was assumed as the sum of rupture front arriving at the most distant subfault from hypocenter and the source duration of a single subfault (source duration of a single subfault was determined from average slip based on scaling relationships and experiential slip velocity). Velocity structure for Green’ s functions were set based on the IASP91 model and the CRUST2.0 model. We used the ABIC [Akaike, [1980]] for temporal and spatial smoothing constraints, and the hyperparameters were set so that ABIC value becomes minimum. Maximum rupture speed was set experientially at 0.70 times of S-wave velocity of near hypocenter. Event magnitude for preset parameters based on scaling relationships was selected from the magnitude +0.0, +0.1, +0.2, +0.3 of Mw (by JMA CMT solution) or Mww (by USGS W-phase moment tensor), and finally we selected event magnitude for preset parameters so that ABIC value become minimum.

3. Verification Methods
(1) We compared aftershock distribution with slip distribution.
(2) We compared seismic moment estimated by aftershocks with slip distribution (seismic moment release).
(3) We compared tsunami source area with slip distribution.

4. Results
Rupture area analyzed by automatic source process analysis located in and around aftershock area for many events. Large aftershock tended to occur adjacent to rupture area. Seismic moment estimated by aftershocks and seismic moment release from main shock were complementary to each other for some events.

Acknowledgement
We thank IRIS for providing the broadband waveform data and IASP91 model. We also thank USGS for providing event parameters. We also use the CRUST2.0 model.

Keywords: Automated Source Process Analysis, Scaling Relationships, Aftershock Distribution

Dynamic rupture simulations for the 2016 Tottoriken-chubu earthquake

*Keisuke Sato[1], Shoichi Yoshioka[2], Hideo Aochi[3,4]

1. Graduate School of Science, Kobe University, 2. Research Center for Urban Safety and Security/Graduate School of Science, Kobe University, 3. Ecole Normale Superieure Paris, Geological Laboratory, Paris, France, 4. Bureau de Recherches Geologiques et Minieres, Orleans, France

In this study, we performed dynamic rupture simulations for the 2016 Tottoriken-chubu earthquake (M6.6). We used a boundary integral equation method, and supposed slip-weakening law as a frictional constitutive law. We assumed a vertical rectangular fault plane whose depth of the upper edge is 0.5 km, the fault size is 19.5 km (along strike)×18 km (down dip), and left lateral faulting. We also assumed a rupture initiation point coincided with its hypocenter (Hi-net automatic processing hypocenter), and the rupture spread from this point. In this study, we attempted to obtain spatial distributions of initial stress and critical slip weakening distance in the slip-weakening law, which can fit better the slip distribution obtained from inversion analysis of the observed seismic waveforms performed by Kobayashi et al. (2016). The final slip distribution obtained from the inversion analysis has an area whose slip amount is very large just above the hypocenter, reaching 1.3 m. In addition, the large slip, reaching 1.27 m, has completed within 1 s (0 s is rupture initiation time).
Firstly, we performed a simulation, assuming uniform dynamic parameters on the fault plane with initial stress of 10 MPa, critical slip weakening distance of 0.25 m, peak stress of 20 MPa, and residual stress of 0 MPa. The simulation shows that the whole area slipped, reaching 4.4 m. We found that it was impossible to explain the inverted slip distribution using uniform dynamic rupture parameters. Therefore, we introduced heterogeneity of dynamic rupture parameters on the fault plane.
We divided the fault plane into two areas, referring to the inverted slip distribution; one is the area with a large slip amount, and the other is the surrounding one with a small slip amount. We assumed that residual stress was 0 MPa, and peak stress was 20 MPa in both areas. Here, we estimated initial stress in these two areas, by fixing the values of critical slip weakening distance. For this purpose, we assigned initial stress of 2 MPa in the surrounding area of small slip, and varied initial stress value from 5 MPa to 15 MPa in the area of large slip. We attempted to obtain an initial stress value so as to minimize the residual between the simulated and inverted final slip distributions by a try-and-error method. As a result, we obtained 10 MPa as the optimal initial stress value in the area of large slip.
Next, we attempted to estimate spatial distribution of critical slip weakening distance values. For this purpose, we assumed the value to be 0.25 m in the surrounding, and divided the area of large slip into four areas in the depth direction (the deepest one included the rupture initiation point). We varied critical slip weakening distance value from 0.25 m to 0.30 m in these four areas. We attempted to obtain critical slip weakening distance values so as to minimize the residual between the simulated and inverted slip distributions at every 1 second by a try-and-error method. As a result, we found there are a trend that the value of critical slip weakening distance become larger toward the direction of the ground surface. Comparing the inverted slip distribution with obtained heterogeneity in initial stress and critical slip weakening distance on the fault plane, we found that an initial stress value in the area of large slip was larger than that of the surrounding, and a critical slip weakening distance value was the smallest in the area including the rupture initiation point than the other upper three areas.

Keywords: dynamic rupture simulation, Tottoriken-chubu earthquake

Simulation of Great Earthquakes along the Nankai Trough: An Attempt at Simulation of Heterogeneous Slip Deficit Rate Distribution and Slip Distributions of the Showa Tonankai / Nankai Earthquakes

*Fuyuki Hirose[1], Kenji Maeda[1], Kenichi Fujita[1], Akio Kobayashi[1]

1. Seismology and Tsunami Research Department, Meteorological Research Institute

1. Introduction

Recently, Yokota et al. [2016, Nature] and Nishimura et al. [2016, AGU] estimated heterogeneous slip deficit rate distributions on the plate boundary along the Nankai trough using both land based GNSS and offshore GPS/A data. We intend to simulate not only the heterogeneous slip deficit rate distribution but also slip distributions of the Showa Tonankai / Nankai earthquakes relatively well known [Baba & Cummins, 2005, GRL] using a three-dimensional earthquake cycle model based on the rate- and state-dependent friction law with heterogeneous frictional parameters on the plate interface along the Nankai trough.

2. Parameter setting

We set frictional parameter a = 0.005 in reference to Sawai et al. [2016, GRL]. The seismogenic zones for which (a-b) is negative are within the depth ranging from trough to 30 km. We used larger effective normal stresses (35-60 MPa) at the plate interface off Shikoku and Tokai districts than the 30 MPa we used elsewhere. We set characteristic displacement L in 0.05-0.20 m on slip distributions of the Showa Tonankai / Nankai earthquakes and in 7.5 m on regions corresponding to small slip deficit rate distributions. The plate convergence rate we used was 5.5 cm/y in the western part of the study area, decreasing eastward from the Kii Peninsula to 1.0 cm/y in the eastern part of the study area [Nishimura et al., 2016, AGU].

3. Results

Preliminary results showed that Mw7.9-8.6 great earthquakes occur with recurrence interval of 90-120 years. We found various rupture patterns as follows, 1: stop off Omaezaki (Hoei eq. type), 2: whole (Ansei Tokai eq. type), and 3: stop off Lake Hamana (Showa Tonankai eq. type) in eastern area, and 4: whole including Hyuganada (Hoei eq. type), 5: off Shikoku district (Ansei Nankai eq. type), and 6: beneath coast of Shikoku (Showa Nankai eq. type) in western area. Occurrence interval between Tonankai and Nankai earthquakes were 0.7-1.6 years. We also found small slip deficit rate distributions off Kii peninsula and off eastern Shikoku district during interseismic periods. Thus, we could roughly simulate the heterogeneous slip deficit rate distribution and slip distributions of not only the Showa Tonankai / Nankai earthquakes but also other historical earthquakes. However, it is necessary to try parameter tuning further because we could not simulate historical occurrence timing.

Keywords: Nankai trough, Simulation, Slip deficit rate distribution, Showa Tonankai / Nankai Earthquakes

Afterslip distribution of the 2003 Tokachi Earthquake and the 2004 Kushiro Earthquakes using poroelastic and viscoelastic media

*Takuma Kobayashi[1], Toshinori Sato[1]

1. Graduate School of Science, Chiba University

1. Introduction

It is important for obtaining frictional properties of plate boundaries to estimate coseismic and afterslip distributions of large interplate earthquakes. Afterslip may trigger another earthquakes, such as the 2004 Kushiro Earthquakes after the 2003 Tokachi Earthquake, and 3/11 main shock of the 2011 Tohoku Earthquake after 3/9 pre-shock. Surface deformation after large earthquakes includes displacements due to afterslip, viscoelastic relaxation, and poroelastic rebound. To determine afterslip distribution correctly, we need to estimate effects of viscoelastic and poroelastic responses. This presentation will show afterslip distribution of the 2003 Tokachi and 2004 Kushiro Earthquakes estimated from GNSS data using viscoelastic and poroelastic media, and discuss relationship between afterslip of the 2003 event and the 2004 events.

2. Data and method

We used daily F3 coordinate values of GNSS control stations from the GSI. We calculated the poroelastic deformation from the surface deformation under two conditions, drained and undrained, in terms of the elastic properties. We consider not only viscoelastic responses of coseismic slip but also viscoelastic responses of afterslip (for detailed method, see Lubis et al. GJI, 2013).

3. Results

The afterslip with poroelastic and viscoelastic media concentrates deep and shallow parts of plate interface at the eastern adjoining area of 2003 Tokachi Earthquake. This distribution of the afterslip spreads eastern side of the coseismic slip area of the 2004 Kushiro Earthquakes, and avoids the 2004 coseismic slip area. No slip area exists at the western side of the 2004 coseismic area. This area has no slip even after the 2004 events.

Acknowledgements

We used daily F3 coordinate values of GNSS control stations from the GSI.

Keywords: Afterslip, poroelasticity, viscoelasticity, 2003 Tokachi Earthquake, 2004 Kushiro Earthquakes

Comparison between postseismic slip immediately after large earthquakes in northeastern Japan

*Shunsuke Morikami[1], Yuta Mitsui[2]

1. Department of Geosciences, Shizuoka University , 2. Faculty of Science, Department of Geosciences, Shizuoka University

In general, postseismic deformation after large earthquakes consists of afterslip and asthenospheric viscoelastic relaxation. Many studies have estimated both effects from year-scale data. Alternatively, we focus on temporal evolution of postseismic deformation, which is almost due to afterslip, following large interplate earthquakes in northeastern Japan (2003 Tokachi-oki, 2005 Miyagi-oki, 2011 Tohoku-oki (March 9), and 2011 Tohoku-oki (March 11)). We obtain surface deformation data at an interval of 30 seconds about 2 days after the earthquakes, from RINEX files of GNSS data, using GSILIB. We invert slip velocities of sub faults at the plate interface from the surface deformation data. First, we find that early afterslip velocities positively correlate with magnitude of the mainshock. Second, we find that the early afterslip velocities are approximately 4 orders of magnitude lower than mean seismic slip velocities of their mainshock. Next, the early afterslips tend to decay almost linearly with time during the investigation periods.

Keywords: afterslip, GNSS, slip velocity

Reestimation of pore fluid pressure fields in the region with intensive swarm activity around Mt. Ontake volcano

*Toshiko Terakawa[1]

1. Earthquake and Volcano Research Center, Graduate School of Environmental Studies, Nagoya University

Overpressurized fluids in the Earth’ s crust have been increasingly implicated to play an important role to earthquake generation by decreasing fault strength (e.g., Hubert and Rubey, 1959). However, it is difficult to directly measure pore fluid pressures in the crust. The focal mechanism tomography (the FMT) is an inversion method to estimate 3-D pore fluid pressure fields by mapping focal mechanism solutions (fault strike, dip angle, and slip angle) of seismicity on the 3-D Mohr diagram for a given tectonic stress field (Terakawa et al., 2010). Validity and applicability of the method are demonstrated by analyzing seismicity induced by fluid injection experiments (where the history of fluid pressures is known) in the Basel Enhanced Geothermal System, Switzerland (Terakawa et al., 2012; Terakawa 2014). On the other hand, in applications of the method to natural earthquakes there was no way to validate results of pore fluid pressures (Terakawa et al., 2010; Terakawa et al., 2013).
In this study we reevaluated the 3-D pore fluid pressure field in the frank of Mt. Ontake in Terakawa et al. (2013). The previous study applied the FMT method to microseismic activity around Mt. Ontake, and estimated overpressureized fluid reservoirs with a peak of 100-150 MPa (with estimation errors of 20 MPa) at depths between 5 and 12 km in the southeast and east franks of the mountain, assuming a tectonic stress field with 10-20 km resolution inferred from events with M > 3 (Terakawa and Matsu’ ura, 2010). In this study we analyzed the same data set as that in Terakawa et al. (2013), assuming a regional stress field with 5 km resolution inferred from smaller events with M > 1 (Terakawa et al., 2016). The pore pressure field obtained in this study is consistent with the former one in the north frank of Mt. Ontake, but discrepancy is large in the southeast and east franks. The peak pore fluid pressure in this study is by > 30 MPa smaller than the former one. In the southeast and east franks difference of the two stress pattens assumed in the two analyses is the largest, although in the two stress patterns the maximum compressive principal stress axes are commonly in the direction of the northwest-southeast. The estimation errors in pore fluid pressures are attributed to both accuracy of the stress pattern and focal mechanism solutions. The level of the pore fluid pressures in the previous study may be overestimated. We reconsider the estimation errors of the stress patterns, and estimate appropriate pore pressure triggering swarm activity.

Keywords: pore fluid pressures, earthquake, stress field

Stress condition around M6.5 earthquake fault of the 2016 Kumamoto earthquake sequence

*Ayaho Mitsuoka[1], Satoshi Matsumoto[2], Yusuke Yamashita[3], Manami Nakamoto[4], Masahiro Miyazaki[3], Shin'ichi Sakai[5], Yoshihisa Iio[3], Group for urgent joint seismic observation of the 2016 Kumamoto earthquake

1. Kyushu University, 2. Institute of Seismology and Volcanology, Faculty of Sciences, Kyushu University, 3. Disaster Prevention Research Institute, Kyoto University, 4. National Institute of Polar Research, 5. Earthquake Research Institute, The University of Tokyo

The 2016 Kumamoto earthquake sequence occurred at Hinagu and Futagawa fault zones under tectonic stress condition of strike slip or normal fault type. First large earthquake with magnitude 6.5 on April 14, 2016 was located at Hinagu fault zone with high seismic activity prior to the event. The stress condition around the fault zone is important to understand the generation of the earthquake. Especially, it is a key factor estimating the spatial variation of stress field at the depth of the hypocenter.
In this study, we estimated the deviatoric stress field and the stress ratio around Hinagu fault zone from focal mechanisms. We used the method estimating it from seismic moment tensor data (Matsumoto, 2016). The data were selected from focal mechanisms of earthquakes occurring from May 2016 to December 2016 at a depth range of 0-20km. We found that the stress field with strike-slip fault regime at the 0-5km depth area. This principal direction is similar to commonly observed in Kyushu Island, Japan. However, the stress field in the area deeper than 5km was in normal fault regime. The maximum principal compressional stress was close to the moderate one at the area. This area corresponds to the co-seismic large slip area estimated from the kinematic waveform inversion of strong motion data (Asano and Iwata, 2016). This suggests that the spatial change in the stress could be caused by decreasing the differential stress at the area deeper than 5km. The stress field around Hinagu fault zone was in strike-slip regime before the occurrence of the M6.5 event and changed to normal fault stress type due to the slip of the event.

Searching significant displacement zone of Orkney earthquake fault by forward and inversion analysis with strain data observed at very close distance

*Tatunari Yasutomi[1], Hiroshi Ogasawara[2], Akimasa Ishida[2], Hiroyuki Ogasawara[2], Raymond Durrheim[3], Alex Milev[4], Makoto OKUBO[5], Teruhiro Yamaguchi[6], James Mori[1]

1. Kyouto university, 2. Ritsumeikan university, 3. Univ.Witwaterarand,South Africa, 4. CSIR,South Africa, 5. Kouchi university, 6. Hokkaidou university

The largest event recorded in a South African gold mining region, a M5.5 earthquake took place near Orkney, South Africa on 5 August 2014. This is one of the rare events as the main- and after-shocks were recorded by 46 geophones and 3 Ishii borehole strain meters at 2 - 3 km depths with epicentral distances, delta < several km, and 17 surface strong motion meters with delta < 20 km. The upper edge of the planar aftershock activity dipping almost vertically was only some hundred meters below the sites where the strainmeters were installed. As the M5.5 seismic rupture is located within a range drillable from gold mine workings at depth, ICDP approved a project to drill into the seismogenic zones. Moyer et al. (2016 SCEC) inverted surface strong motion data, suggesting significant fault slip even at the mining horizon, while there was no seismic rupture mapped or there were three strainmeters installed. So, the three strainmeters can contribute to constrain the configuration of the seismic rupture. As population of the aftershocks varies in space significantly, we expect a possibility to discuss a relationship the fault slip and the aftershocks.
These strainmeters were apart each other about 150 m only. However, their strain changes had different polarities while the other M4 strain changes with a similar hypocentral distance was the same. So, this information can constrain the location and configuration of the M5.5 fault critically.
First, we conducted a forward analysis by assuming a point source with the mechanism same as macroscopic one of the M5.5 faultingat a distance of a few km. However, no difference in polarity in strain change was seen, suggesting that the effect of a finite size of the source with an edge much nearer than the point source had to be taken into account. We are attempting to invert the slip distribution on a source with a finite size together with surface strong motion data. We will report on the results at the meeting.

Keywords: South Africa, induced earth quake, inversion

Terzaghi's theory of consolidation and precursory time of earthquakes

*Naoto Kaneko[1], Hiroyuki Nagahama[1]

1. Tohoku University

In general, the greatly repetitive shearing stress during earthquakes causes ground deformation and subsidence. As a result, severely ground deformation and liquefaction were induced during the 1995 Kobe earthquake (M 7.2) and Tokachi-Oki Earthquake (M 8.0). Settlement of ground can be explained by Terzaghi’ s theory of consolidation in the field of soil mechanics. Terzaghi introduced the concept of strain to the consolidation equation in the theory. On the other hand, the diffusion-like equation for earthquake prediction can explain precursory phenomena such as crustal movement and electrical resistivity closely link to the relationship between magnitude and precursor time. However, the reason is obscure why derived from the diffusion-like equation in spite of given seismological impact. Accordingly, we noticed the void ratio from the point of view of consolidation rather than the equation by the concept of hydrostatic pressure. In the beginning, we referred on the assumption that the critical state soil mechanics. Therefore, this consolidation idea (to relate void ratio and dilatancy) can effectively explain the electrical resistivity composed in saturated ground. Conventionally, the field of earthquake and consolidation is independently, however we would like to receive the baton from both fields and previous research for the goal of earthquake prediction from this study. Here, we indicate essence on saturated ground settlement process links to above.
The part of the present study is published in Kaneko, N., and Nagahama, H. (2016), Theory of consolidation and precursory time of earthquakes, IOSR Journal of Mechanical and Civil Engineering, 13(4), Ver. V, pp. 44-46., doi: http://dx.doi.org/10.9790/1684-1304054446

Keywords: Consolidation, Dilatancy, Earthquake, Porous medium equation, Precursory time

Moment tensor analysis of acoustic emissions induced by hydraulic fracturing in laboratory experiments

*Makoto Naoi[1], Kengo Nishihara[1], Kazune Yamamoto[1], Shunsuke Yano[1], Wataru Fujito[1], Youqing CHEN[1], Tsuyoshi Ishida[1], Hironori Kawakata[2], Takashi Akai[3], Isao Kurosawa[3]

1. Kyoto University, 2. Ritsumeikan University, 3. Japan Oil, Gas and Metals National Corporation

Hydraulic fracturing has been used for the development of Enhanced Geothermal reservoirs and Shale Gas/Oil reservoirs in order to stimulate reservoirs by producing artificial fractures. Microseismic observation is often employed to monitor the hydraulic fracturing. Some field observations suggested that shear events were dominated (e.g., Maxwell, 2013), although an open crack along the maximum compression axis is predicted by stress concentration around a circular hole in elastic medium. Focal mechanisms of earthquakes induced by hydraulic fracturing is important because, for example, proppants are injected so as to prevent closing cracks in Shale Gas/Oil Reservoirs and they should enter open cracks more easily. It is however difficult to constrain focal mechanisms of induced earthquakes in such fields due to insufficient network coverage.
In the present study, we conducted hydraulic fracturing laboratory experiments under uniaxial loading by using 7 granite samples, and monitored acoustic emissions (AE) by a 16-channel AE monitoring system, estimating their seismic moment tensors. Generally, moment tensor analysis, in which accurate measurements of waveform amplitudes are necessary, is difficult for AE data owing to unknown and complex sensor characteristics such as sensor sensitivity depending on sensor coupling. In this study, we estimated the influence of coupling of individual AE sensors in each experiment by using an approach similar to Kwiatek et al. (2013), and estimated moment tensors by using calibrated AE amplitudes. We classified the obtained moment tensor solutions into isotropic, double couple and CLVD dominant solutions on the basis of the decomposition method of Knopoff and Randall (1970). The shear-dominated events occupied 20%-55% whereas CLVD dominated events indicating open-mode cracks occupied 10–20%. In addition, T-axes of the CLVD dominated events (corresponds to open axis of the corresponding open cracks) were consistent with that of the open cracks predicted by stress concentration nearby a circular hole.

Keywords: Acoustic Emission, Hydraulic fracturing, Moment tensor

Response of Transmitted-wave Amplitude to a Biaxial Compressive Experiment

*Miyuu Uemura[1], Yoshihiro Ito[2], Kazuaki Ohta[2], Ikuo Katayama[3]

1. Kyoto University, 2. Disaster Prevention Research Institute, Kyoto University, 3. Hiroshima University

Active and passive seismic monitoring approaches, such as active seismic survey and seismic interferometry, for phenomena on subducting plate interfaces, especially slow earthquakes, are one of technically feasible ways to measure strain accumulation and release in subduction zones. A laboratory experiment is one of the effective approaches to unravel the mechanism. Some previous studies, reporting on laboratory experiments using rocks, have described results on the response of amplitude and velocity reductions to failure occurrence (e.g., Lockner et al., 1977; Yoshimitsu et al., 2009). Additionally, some previous studies, which imitated slow slip events in the laboratory setting, have reported on velocity reductions before and after a slow stick-slip event (Nagata et al., 2008; Scuderi et al., 2016). Here we show a response of amplitude in transmitted waves to the occurrence of slow slip in a biaxial compressive experiment.

We used three stainless steel blocks (a center block and side blocks) and held Ca^{-} montmorillonite powder as simulated fault gauge between each of the center blocks and the side one. We used piezoelectric elements as transmitters, putting them on the center block, while putting three receivers on the side blocks, which are aligned along the loading direction and placed at an interval of 10 mm. We ran a series of slide-hold-slide experiments. In the initial run, the center block slid first at 1.5 μm/s for 5 mm, and the block was then held stationary for 1000 s. In the second run and the third run, the block was held stationary for ~3600s and ~32500s on second and third runs, respectively. The sliding was resumed with the same velocity and the same displacement as the first run. After the third hold, the sliding was continued with the same velocity until reaching 2mm of displacement, thus achieving 17 mm displacement in total. We recorded the transmitted waveforms for every 1mm displacement during the sliding period, and every 100 seconds during the holding period, as well as just before and after the holding period.

The preliminary results show that the transmitted-wave amplitude recovered in accordance with the logarithm of the elapsed time during the hold, and that the rate of amplitude reduction is on average about ~10% just after holding periods at all the receivers. The recovery and reduction of amplitude observed for the transmitted waves could be due to change of frictional contact on interface due to the occurrence of sliding.

Keywords: biaxial compressive test, slow slip

Temperature-dependent frictional strength of dolerite in an argon atmosphere

*yokoyama yuuki[1], Hiroki Murayama[1], Kyuichi Kanagawa[1], Michiyo Sawai[1]

1. Chiba University

Since 1990’s, high velocity friction experiments (up to several m/s) on many types of rocks have revealed that frictional strength significantly decreases with increasing slip rate at seismic slip rates (e.g., Tsutsumi and Shimamoto, 1997; Di Toro et al., 2011). Coseismic weakening mechanisms are due to temperature rise including flash heating, melt lubrication or thermal pressurization (e.g., Rice, 2006; Hirose and Shimamoto, 2005). Although the important role of temperature rise in fault motion are widely recognized, there is just a few studies which investigated the effect of temperature on frictional properties at intermediate to high slip rates (e.g., Noda et al., 2011). Yao et al. (2015) conducted the high velocity friction experiments using host blocks with different thermal conductivity values, and reported that the amount of slip-weakening increases with decreasing thermal conductivity values of host blocks. This implies that an ambient fault temperature has a large effect on the frictional strength at the coseismic slip rates. We therefore performed friction experiments at a wide range of temperatures and slip rates, and investigated the effect of temperature on the friction coefficient (μ).
Experiments were conducted on dolerite (Belfast, Northern Ireland) using a rotary shear deformation apparatus at Chiba University. Dolerite samples were sheared at a normal stress of 1 MPa, slip rates of 1 to 300 mm/s, slip displacements of 10 - 20 m at each slip rate and temperatures of 20 - 500°C in an argon atmosphere with an oxygen concentration of 0.2 %. A high-frequency induction coil surrounding the sample holders is used to heat up the sample holders and the rock samples.
At 20°C and 100°C, the dolerite showed velocity weakening at the range of slip velocities 1 - 30 mm/s with μ ranging 0.81 - 0.83 at 1 mm/s and of 0.73 at 30 mm/s. Whereas at high temperatures >300°C, friction is almost constant (μ = 0.81 - 0.85) at < 30 mm/s. At 100 mm/s, the behavior is slight velocity strengthening at 20°C and 100°C with μ = 0.75 - 0.79 and clear velocity-weakening at more than 300°C with μ = 0.67 - 0.76. At 300 mm/s, the dolerite showed strong velocity weakening at all temperatures investigated. The amount of weakening (i.e., the drop in friction, $\Delta\mu$) increases with increasing temperature ($\Delta\mu$ = 0.1 - 0.38). Thus, the frictional properties of dolerite are affected by not only slip rate but also the ambient temperature. Our results suggest that rocks at depths are energetically favored for earthquake ruptures to propagate deeper.

Keywords: friction, temperature dependence, dolerite

Dynamic water permeability change of simulated fault induced by moderate velocity friction

*Wataru Tanikawa[1]

1. Japan Agency for Marine-Earth Science and Technology, Kochi Instutute for Core Sample Research

Co-seismic events induce sudden changes in pore pressure, flow rate, and fluid chemistry at depth. These temporal transitions could be explained by water permeability changes of fault zones at depth during earthquakes, and change in permeability in fault zone also plays an important role in dynamic processes. Considerable change of permeability may occur during the transition from coseismic to post-seismic period, though the change is not well documented. Therefore, I designed the laboratory system to measure the change of water permeability during low to high velocity friction tests using simulated fault rocks. Similar permeability-friction tests were conducted in the past studies (Tanikawa et al., 2012, 2014). However, the previous tests were conducted by using nitrogen gas as pore fluid, and slip rate was not so high compared to dynamic fault motions.
In this study, Belfast dolerite and Aji granite were used as test specimens. For each experiment, two 20-mm-long hollow cylindrical specimens with 40 mm and 16.5 mm outer and inner diameters, respectively, were used. To measure the permeability, radial flow from the inner wall to the outer wall of the specimen was induced by applying a differential pre pressure between inner and outer walls. 0.1 to 0.8 MPa of constant pore pressure was applied from the inner wall, and water flowing out from the outer wall was released to the atmosphere. I applied constant normal stress of 2 MPa and constant rotation speed from 0.1 to 100 rpm (0.001 to 0.1 m/s) for a slip displacement of 1 to 10 m.
The result shows that permeability (flow rate) increased suddenly at the onset of sliding by a factor of more than two, and the rate of increase was nearly proportional to permeability before sliding. After sliding, permeability was decreased gradually with time, and had almost stabilized within few minutes. To compare the permeability before and after sliding, higher velocity friction (>0.03 m/s) results in the increase of permeability, and slower velocity friction induced the permeability reduction. This transition appears to be related to velocity dependent friction behavior, as velocity weakening was observed at above 0.03 m/s of slip velocity. Permeability reduction and velocity weakening behavior at slower velocity regime is probably explained by gouge compaction and gouge friction. On the other hand, high velocity friction will produce thermal pressurization, flash heating, and thermal cracking, therefore, the transition process of water permeability for high velocity friction would be more complicated than slow velocity friction.

Keywords: permeability, friction coefficient, fault

Frictional strength of agate at intermediate slip rates in air and argon atmospheres

*Hiroki Murayama[1], Kyuichi Kanagawa[1], Michiyo Sawai[1], Takehiro Hirose[2]

1. Graduate School of Science, Chiba University, 2. Kochi Institute for Core Sample Research, Japan Agency for Marine-Earth Science and Technology

Frictional strength of quartz rocks is known to be extraordinary low at subseismic slip rates ranging from 1 mm/s to 10 cm/s, and this weakening has been ascribed to the hydration of comminuted material, i.e., silica gel formation (e.g., Goldsby and Tullis, 2002; Di Toro et al., 2004; Hayashi and Tsutsumi, 2010). If so, frictional strength of quartz rocks at dry conditions would not significantly decrease at those slip rates, because the hydration of comminuted material would be prevented. In order to testify this hypothesis, we conducted rotary-shear friction experiments on agate samples at a normal stress of 1.5 MPa and intermediate slip rates of 1 cm/s and 10 cm/s, i.e., at the same conditions as those of experiments done by Hayashi and Tsutsumi (2010), but in humid-air and dry-argon atmospheres, and compared frictional strengths in humid and dry conditions.
At a slip rate of 1 cm/s, frictional strength in both atmospheres did not change much with displacement so that friction coefficients after displacements of ≈180 m were as high as ≈0.7. In contrast at a slip rate of 10 cm/s, frictional strength in both atmospheres significantly decreased with displacement, and friction coefficients after displacements of ≈250 m became as low as ≈0.25, although significant fluctuations in frictional strength were observed throughout the experiments. Thus our results show that frictional strength of agate at a given slip rate does not differ between humid and dry conditions, and therefore cast doubt about weakening of quartz rocks caused by the hydration of comminuted material. Since we observed flashes along the slip surface during experiments at a slip rate of 10 cm/s, significant weakening of agate at this slip rate is likely due to the flash heating of asperities. We monitored thermal images during experiments in air at both slip rates of 1 cm/s and 10 cm/s, and will also report the relationship between frictional strength and the slip-surface temperature.

Keywords: frictional strength, agate, in air, argon atmosphere

evolution of localized shear texture on a simulated fault surface of quartz rocks during slip-weakening process at a intermediate slip velocity

*Hirotaka Iida[1]

1. Graduate School of Science, Kyoto University

Siliceous rocks such as novaculite and quartzite display dramatic weakening of frictional strength at slip velocities of >1 mm/s [Goldsby and Tullis, 2002; Di Toro et al., 2004]. It is known that hydrated amorphous silica gouges form on the fault surface in the intermediate-high velocity frictional slip [Hayashi and Tsutsumi, 2010]. Goldsby and Tullis [2002] suggested that the silica gel layer made of very fine amorphous silica particles causes the frictional weakening. However, there are few reports focused on the state of these silica gouges during the slip-weakening process. In this study, to better understand the state of the fault surface during the slip-weakening, SEM observations of the fault surface and section and XRD analyses of the silica gouge were performed.
All the experiments in this study were conducted using a rotary-shear, intermediate-to high-velocity friction testing machine in Kyoto University. The samples used for the friction experiments were single crystal of quartz (a synthetic crystal). A pair of solid cylinders with a ring-shaped end surface (inner and outer diameter of 5 mm and 25 mm) was cored from the samples. Experiments were carried out at a constant normal stress of 1.5 MPa and a slip velocity of 105 mm/s condition.
As an experimental result, slip-weakening occurred at the initial 0.2–0.3 m of the sliding and the value of friction coefficient dropped from the peak value 0.6 to residual value 0.2. The peak friction showed log(t) healing [Dieterich, 1972]. Whole of the fault surfaces of the specimens were completely covered with white, fine-grained gouges after the experiments. SEM observations showed that 100–300 μm size of plate-like structures had been formed on the surface. The surfaces of these structures were very smooth and flat. These structures were teared from the surface into a shear direction. SEM observations of the fault section revealed that a continuous shear plane had been formed at the center of the fault zone. Along and parallel to this shear plane, approximate 1.5 μm-thick layers had piled up and formed foliation structures. Similarities in size and direction of the planes suggest that these piled layer structures should correspond to the plate-like structures found on the fault surface.
XRD analyses of the fault gouge revealed that amorphization of gouges had already been occurred during the slip-weakening.

Keywords: quartz, weakening, structure, amorphous, healing, gouge

Cathodoluminescence spectra properties of recrystallized quartz in mylonite.

*Kotaro Tano[1,2], Takuto Kanai[1], Shunsuke Watanuki[1], Hideo Takagi[1]

1. Waseda Univ., 2. Japan Oil, Gas and Metals National Corporation

Quartz has characteristics of cathodoluminescence (CL) emission due to structural defects in the crystal and presence of impurity elements. Previous studies have been reported that emission intensity decreases due to mylonitization based on the observation of CL images (Shimamoto et al., 1991; Morales et al., 2011; Kidder et al., 2013). However, no research has been reported on examining the influence of mylonitization by separating the CL spectrum for each emission factors. In this study, CL spectra of quartz grains in mylonite were measured using SEM-CL in order to elucidate the influence of quartz on the CL spectrum by shear deformation. CL spectra of quartz grains in the mylonites from Iragawa mylonite zone (Aomori Prefecture, NE Japan) and along the Median Tectonic Line (MTL) in Mie Prefecture, SW Japan were measured and examined characteristics of each separated spectra. Spectra of quartz grains have two peaks (around 420 nm and 620 nm) or only one peak (around 620 nm). Principal component analysis (PCA) of CL spectra data was examined in order to extract potential factors which influence the CL spectra. As the result of the PCA, the first principal component (PC1) and the second principal component (PC2) represent the emission intensity and the intensity ratio between the blue side (380–450nm) and the red side (580–650nm), respectively. Since the PC2 score is influenced by the overall emission intensity, the spectra of each sample are normalized as the areas become equal. The normalized spectrum was multiplied by the eigenvector of PC2 to obtain the score (PC2') as PC2 score. After that, measured spectrum was fitted by nine Voigt functions (mixed Voigt function) and parameters of each Voigt functions were estimated by the least squares method and calculated mixing coefficients for each peak. The center wavelength of each Voigt function was set to nine (380, 420, 450, 500, 580, 620, 650, 705 and 730-800 nm) whose emission factors are summarized by Hunt (2013).
PC2’ score and the mixing coefficients indicated that the emission intensity on the red side are increasing together with decreasing grain size of recrystallized quartz across the Iragawa mylonite zone and the MTL mylonite zone. The deformation temperatures estimated by quartz LPO do not show conspicuous change across the Iragawa mylonite zone (Watanuki et al., 2017), so the clear change of PC2’ does not depend on the change in the deformation temperature. The PC2’ results can be therefore interpreted by the effects of the lattice defects (e.g. Al or Ti substitute decrease, or non-brigding oxygen hole center: NBOHC increase associated with strengthening mylonitization. Especially NBOHC is attributed to OH^- bonding defect (Götze et al, 2001). Therefore, this defect was presumably increased by mylonitization. We need to clarify exact kind of lattice defects in recrystallized quartz in strongly deformed mylonites.

Reference

Götze, J., Plötze, M., and Habermann, D., 2001, *Mineralogy and Petrology*, **71**, 225-250.
Hunt, A. M. W., 2013, *Jour. Arch. Sci.*, **40**, 2902-2912.
Kidder, S., Avouac, J. P., and Chan, Y. C., 2013, *Solid Earth*, **4**, 1-21.
Morales, L. F. G., Mainprice, D., Lloyd, G. E., and Law, R. D., 2011, *Geol. Soc. London Spec. Publ.,* **360**, 151-174.
Shimamoto, T., Kanaori, Y., and Asai, K., 1991, *Jour. Struct. Geol.* **13**, 967-973.
Watanuki, S., Kanai, T., Saka, H., Takagi, H., 2017, *Jour. Geo. Soc. Japan*, **123**, in press.

Keywords: Quartz, Cathodoluminescence, Mylonite

Raman spectra of carbonaceous materials within the black fault rocks in Kodiak accretionary complex

*Asuka Yamaguchi[1], Raimbourg Hugues[2]

1. Atomosphere and Ocean Research Institute, The University of Tokyo, 2. Institut des Sciences de la Terre d'Orleans , Universite d'Orleans

Estimation of frictional heat generated in the principal slip zone (PSZ) of a fault is a key to understand fault mechanics. Recently, analyses on carbonaceous material (CM) such as vitrinite reflectance and Raman spectroscopy, which were widely used as geothermometer, have been applied to fault rocks and products of friction experiments (e.g Sakaguchi et al., 2011; Kitamura et al., 2012; Furuichi et al., 2015; Kaneki et al., 2016; Kouketsu et al., 2017). Raman spectroscopy of CM has an advantage in 2-dimentional mapping, and therefore useful for quantifying high temperature zone along PSZ generated by thermal diffusion of frictional heat. However, distribution of Raman spectra of CM within a PSZ has not considered well. In this presentation, we show the result of Raman spectra of CM within the PSZ of the Pasagshak Point Thrust in the Kodiak accretionary prism. The thrust is characterized by ultrafine-grained black fault rocks (BFR) including weakly molten pseudotachylyte formed during seismic slips (Rowe et al., 2005; Meneghini et al., 2010; Yamaguchi et al., 2014).
Raman spectra were obtained using a Renishaw InVIA Reflex microspectrometer (ISTO-BRGM; Orléans) with 514 nm laser. The laser beam power at sample surface was set to ~0.5 mW. Analysis was performed to traverse internal textures of the BFR. Spectra was decomposed into five peaks, center positions around 1350 cm^{-1} (D1, D3 and D4) and graphite bands centered around 1580-1600 cm^{-1} (D2 and G). Microstructures of the BFR were observed under cathodoluminescence microscope.
Although D1-band develops within the crystalline microlayers of aphanitic BFR, which is thought to be melt-origin pseudotachylyte (Meneghini et al., 2010), development of G-band was not detected even in the crystalline microlayers. This observation suggest that Raman spectra of CM do not reach the equilibrium in the case of short-time heating, as pointed out by Nakamura et al. (2017). An alternative possibility is that Kodiak BFR has formed temperatures of <400 degrees C, without frictional melt.

Frictional Properties and Microstructures of Main Fault Gouge of Mont Terri Rock Laboratory, Switzerland

*Kazuhiro Aoki[1], Kazuyoshi Seshimo[1], Toru Sakai[2], Masao Kametaka[2], Toshihiko Shimamoto[3], Shengli Ma[3], Lu Yao[3]

1. Japan Atomic Energy Agency, 2. Dia Consultants, 3. Institute of Geology, China Earthquake Administration

Friction experiment was conducted on samples of main fault of Mont Terri Rock Laboratory, Switzerland and then microstructures of experimented fragments were observed by a JCM-6000. Samples were taken at the depths of 47.2m and 37.3m of borehole BSF-1, and at 36.7m, 37.1m, 41.4m and 44.6m of borehole BSF-2, which were drilled from the drift floor at the depth of 260m from the surface. Friction experiment was conducted on above 6 samples using a rotary shear low to high-velocity friction apparatus at Institute of Geology, China Earthquake Administration in Beijing at a normal stress of 3.95 to 4.0 MPa and at slip rates ranging 0.2 microns/s to 2.1mm/s. Cylindrical specimens of Ti-Al-V alloy with 40 mm in diameter were used as rotary and stationary pistons and the alloy pistons exhibit similar behaviors as host rock specimens. A Teflon sleeve was used around the piston to confine the sample during a test.

Main experimental results are summarized as follows.
1) Mud rocks in Mont Terri drill holes (BFS-1, BFS-2) have the following ranges of steady-state or nearly steady-state friction coefficient μ_{ss}: μ_{ss} *(wet)*: mostly 0.1~0.3, μ_{ss} *(dry)*: mostly 0.5~0.7
Dry gouges have about twice as large friction coefficients than wet gouges.
2) However, fault rock (37.3 m, BFS-1) with scary fabric has: μ_{ss} *(wet)*: 0.50~0.77, μ_{ss} *(dry)*: 0.45~0.78 (no difference between the two) This is probably because the clay contents of this rock is less (~ 33 %) than those in other rocks (67~73 %).
3) Initial peak friction coefficient μ_p is more or less on the same order of magnitudes as μ_{ss} although μ_p can increase with increasing contact time and cementation in natural environments.
4) Deformed gouges are characterized by well-developed slip zones adjacent to the rotary and stationary pistons, accompanied by slickenside surfaces with clear striations. Those slickenside surfaces are similar to those developed in the drill core samples used in our experiments.
5) Slip zones are unclear in deformed fault rock from 37.3 m (BFS-1), and probably slickenside surfaces form easily in clayey mudrocks.

Keywords: friction experiment, Mont Terri Rock Laboratory, friction coefficient, back scattered electron image

Determination of the deformation conditions of the Shajigami Shear Zone developed in Fukushima Prefecture, northeast Japan, based on deformation microstructures of mylonites

*Shunsuke Watanuki[1], Shuya Hisasue[1], Takuto Kanai[1], Hideo Takagi[1]

1. Waseda University

The Shajigami Shear Zone (Yamamoto et al., 1989) extends NE–SW in the South Kitakami Belt, eastern margin of Abukuma Mountains, northeast Japan. Hisada and Takagi (1992) reported that the granodiorite mylonite indicate a sinistral shear whereas the granodiorite cataclasite and the limestone mylonite indicate a dextral shear. In this presentation, the deformation condition is estimated based on the lattice preferred orientation (LPO) and the grain size distribution of recrystallized quartz of the granodiorite mylonite and calcite of the limestone mylonite are measured using SEM–EBSD.
The granodiorite mylonite is distributed along the Shajigami Fault and mostly overprinted cataclasis. The mylonites show quartz LPO patterns suggesting activity of rhomb <*a*> and/or prism <*a*> system. The microstructures and LPO patterns suggest dislocation creep took place at about 400 ˚C (Takeshita, 1996; Passchier and Trouw, 2005). The mean grain size of recrystallized quartz ranges 13.8–21.1 μm.
The grain size (mean: 16.9–46.9 μm) of recrystallized calcite in the limestone mylonite is minimum along the fault. Asymmetric deformation microstructures indicate a dextral shear, but some calcite porphyroclast preserve a microstructure of former sinistral shear. The LPO is characterized by a maximum of the *c*–axes in the Z direction rotating clockwise (10–20˚). The *a*–axes are distributed within a girdle in the XY plane. The twin geometry of calcite grains indicates the plastic deformation above 200 ˚C (Burkhard, 1993). Hisada and Takagi (1992) estimated the granodiorite cataclasites are formed up to 90 Ma.
In conclusion, the granodiorite mylonites are deformed at about 400 ˚C after 105 Ma (hornblende K–Ar ages; Agency for Natural Resources and Energy, 1990). After the strike–slip inversion, the limestone mylonites and granodiorite cataclasites were formed at 200–300 ˚C up to 90 Ma.

References

Agency for Natural Resources and Energy, 1990, *Agency for Natural Resources and Energy*, 116p.
Burkhard, 1993, *Jour. Struct. Geol.*, **15**, 351–368.
Hisada, T. and Takagi, H., 1992, *Jour. Geol. Soc. Japan*, **98**, 137–154.
Passchier, C. W. and Trouw, R. A. J., 2005, Springer, Berlin, 366p.
Takeshita, T., 1996, *Jour. Geol. Soc. Japan*, **102**, 211–222.
Yamamoto, T., Kubo, K. and Takizawa, F., 1989, *Jour. Geol. Soc. Japan*, **95**, 701–710.

Keywords: Shajigami Shear Zone, Mylonite, Lattice preferred orientation

Distribution and characteristics of fractures in the vicinity of spray fault branching off from out of sequence thrust: a case of the Sengen fault, Miura Peninsula

*Masahiro Muraki[1], Shinichi Uehara[2]

1. The University of Tokyo National Environmental Changes Department of National Environmental Studies Graduate School of Frontier Science, 2. Toho University Faculty of Science Department of Environmental Science

Pore fluid on fault plane influences fault movement. Therefore estimation of fluid behavior of in the vicinity of a fault is important to understand deeply occurrence mechanism of earthquakes. At subduction zones, out of sequence thrusts (OST) often branch off from a decollement zone associated with making accretionary prism. OST is known to be an effective fluid flow path in accretionary prism. Fluid is expressed from deposition by lateral compression associated with making accretionary prism, and may cause high pore fluid pressure. The high pore pressure fluid may flow into cracks in the vicinity fault which are created associated with fault activity. As an evidence of the fluid migration, mineral veins such as calcite have been observed at outcrops along faults. Therefore, to research distribution and characteristics of fractures along OST is important to evaluation of fluid behavior in the vicinity OST. This study reports distribution and characteristics of fractures in the Sengen fault, which is a spray fault branching off from the Jogashima thrust, OST in south Miura peninsula. Paleo-stress conditions and pore pressure were also estimated by applying a paleo-stress analyses method of Yamaji [1] to data of calcite veins orientations in the vicinity fault.
The Sengen Fault is a reverse fault (N 84˚W, 70˚N) A fault core and the vicinity of the Sengen fault is composed of three distinct parts: a black gouge zone of about 1 centimeters thick as main slip surface, a breccia zone of about 20 meters thick on the hanging wall side, and a shear band zone on the footwall side. The gouge zone shows mineral alignment parallel to the fault plane, and the breccia zone exhibits weak mineral alignment in the orientation oblique to the fault plane in microscope scale. Fracture density decreases as a distance from the main slip surface, and when the distance is larger than approximately 100 m, the density is nearly constant. An orientation of a strike of fractures within approximately 100 m from the main slip surface is different from that of fractures which are more than 100 m away from the main slip surface in the hanging wall side, and the orientation of strike of the former is closer to the strike of the Sengen fault. Therefore, a width of damage zone, in which the fault-related fractures are distributed,) was estimated as approximately 100 m. Yamamoto et al. [2] indicated that calcite veins are commonly recognized on the hanging wall side of the fault. Calcite veins were recognized from 80-200 m from the main flip surface on the hanging wall side. A orientations of strikes seems weakly to concentrate around N 50˜80˚E. Paleo-stress analyses estimated the stress field of reverse fault (the maximum principal stress: NNW - SSE) and normal fault (the minimum principal stress: NNE - SSW) in the vicinity of the Sengen fault. Estimated pore pressure ratio for stress field of reverse fault is higher than that for stress field of normal fault

[1] Yamaji (2012) THE JOURNAL OF GEOLOGICAL SOCIETY OF JAPAN, VOL.118 , No 6, p.335-350
[2] Yamamoto et al. (2005) TECTONICS, VOL, 24, TC5008.

Keywords: out-of-sequence-thrust, damage zone, Paleostress analyses, pore pressure

Structural, mineralogical, and geochemical characteristics of an ancient megasplay fault in the Hidakagawa Formation, Kii Peninsula

*Takeaki Ogawa[1], Tsuyoshi Ishikawa[2], Shunya Kaneki[1], Tetsuro Hirono[1]

1. Department of Earth and Space Science, Graduate School of Science, Osaka University, 2. Kochi Institute for Core Sample Research, Japan Agency for Marine-Earth Science and Technology

To understand the slip behavior of large earthquakes along subduction zone, a great deal of effort has been made on the accretionary complex such as the Shimanto Belt. Although extensive investigation along the trench is important, no studies have ever tried to analyze fault rocks in accretionary complex of west coast of Kii Peninsula. Here we focus on mélange unit in the Hidakagawa Formation, outcropped in the Mio region, Wakayama Prefecture. We revealed geological setting and mineralogical and geochemical characteristic by performing the structural description, Raman spectroscopic analysis, mineral composition analysis, and geochemical analyses of major- and trace-element concentrations of the fault rocks and its surrounding rocks.
The burial depth in this region was estimated 3-4 km, also indicating large cumulative displacement along the fault. Granuation of mineral grains and shear foliation were well developed in the slip zone, and high temperature (>350 ˚C) by fluid-rock interaction was estimated along the slip zone. These features were well coincided to those in the megasplay fault. Furthermore, we discuss the slip behavior and the slip parameters.

Keywords: accretionary prism, trace-element, fluid-rock interaction, megasplay fault, Shimanto belt

Prescribed factor of major and trace elements composition presumed by the borehole core sample of Nobeoka thrust

*Hasegawa Ryota[1], Asuka Yamaguchi[1], Yujin Kitamura[2], Tsuyoshi Ishikawa[3], Rina Fukuchi[1], Juichiro Ashi[1]

1. Atmosphere and Ocean Research Institute, The University of Tokyo, 2. Graduate School of Science and Engineering KAGOSHIMA UNIVERSITY, 3. Kochi Institute for Core Sample Research, Japan Agency for Marine-Earth Science and Technology

Megasplay faults branching from plate boundaries at subduction zones are thought to be important sources of earthquakes generating tsunamis. The Nobeoka Thrust is the low-angle thrust which subdivides the Shimanto Belt in Kyushu into the northern (Cretaceous and Paleogene) and the southern (Paleogene to Neogene) subbelts, and is an exhumed analogue of an ancient megasplay fault. The hanging wall and the footwall of the Nobeoka Thrust show difference in lithology and metamorphic grade, and their maximum burial temperatures estimated from vitrinite reflectance analysis are 320~330°C and 250~270° C, respectively. Assuming this temperature gap was made by fault displacement, the total displacement is estimated to be approximately 10 km (Kondo et al., 2005).
Borehole core samples penetrating through the Nobeoka Thrust were collected by the Nobeoka Thrust drilling project (NOBELL) in 2011. Since then, various studies using the borehole core have been performed. In this research, we performed major and trace element composition analysis for each depth of the borehole core collected by the NOBELL, and aim to clarify the nature of fluid-rock interaction along the fault core of the Nobeoka Thrust.
Major and trace element compositions across the principal slip zone (PSZ) of the Nobeoka Thrust were analyzed 38 samples by XRF (Rigaku ZSX) and ICP-MS (Agilent 7700x ICP-MS) respectively, installed at Kochi Core Center (Kochi University/JAMSTEC). As a result of principal component analysis (PCA) on the results of the major element compositions, a decrease in Si and Na with an increase in K is found in the PSZ. This suggests the possibility of hydrothermal alteration reaction (albite to illite) during the faulting process. Fukuchi et al. (2014) showed that the illite crystallinity nearby the PSZ of the Nobeoka Thrust could be affected by hydrothermal alterations in addition to mechanical comminution. We also carried out XRD analysis by using samples for chemical composition analysis. Although quantitative change in abundance of illite was not confirmed, disappearance of albite was detected in the PSZ.
Almost all the elements fluctuated largely just above the PSZ. This observation can be ascribed to high-temperature fluid-rock interaction occurred just above the PSZ, because some of the trace elements sensitively react with high-temperature water. However, more carefully, large abundance of elements characteristic in carbonate minerals (Ca, Mg, Fe, Mn and Sr) occurred at the upper part of the PSZ, while positive anomaly of Cs peak was observed 3 cm below the carbonate-enriched depth. Such discordance in depths of anomalies in each element suggest the existence of more complicated reactions occurred within the PSZ.
Through this study, several effects of fluid-rock interaction during faulting process have been clarified. To strengthen the scope of the findings in this study, it would be beneficial to perform a cross-section analysis of the borehole sample. This will enable us to understand the detailed changes of the element and mineral composition that occurs during faulting.

